XTH20 and *XTH19* controlled by ANAC071 under auxin flow are involved in cell proliferation in incised *Arabidopsis* inflorescence stems

Weerasak Pitaksaringkarn[1], Keita Matsuoka[1], Masashi Asahina[2], Kenji Miura[1], Kimiyo Sage-Ono[1], Michiyuki Ono[1], Ryusuke Yokoyama[3], Kazuhiko Nishitani[3], Tadashi Ishii[1], Hiroaki Iwai[1] and Shinobu Satoh[1,*]

[1]Graduate School of Life and Environmental Sciences, University of Tsukuba, Tsukuba, Ibaraki 305-8572, Japan.

[2]Department of Biosciences, Teikyo University, Utsunomiya, Tochigi 320-8551, Japan.

[3]Graduate School of Life Sciences, Tohoku University, Sendai, Miyagi 980-8578, Japan.

[*]Coreresponding author: Shinobu Satoh

E-mail: satoh.shinobu.ga@u.tsukuba.ac.jp

Telephone and Fax: +81-29-853-4672

Running title: *XTHs* and ANAC071 in Tissue Reunion

SUMMARY

One week after partial incision of *Arabidopsis* inflorescence stems, the repair process in damaged tissue includes pith cell proliferation. Auxin is a key factor controlling this process, and *ANAC071*, a transcription factor gene, is up-regulated in the distal region of the incised stem. Here we show that *XTH20* and the phylogenetically close *XTH19* were also up-regulated in the distal part of the incised stem, similar to *ANAC071*. *XTH19* was expressed in the proximal incision region after 3 days or after auxin application to the decapitated stem. Horizontal positioning of the plant with the incised side up resulted in decreased Pro_{DR5}*:GUS*, *ANAC071*, *XTH20*, and *XTH19* expression and reduced pith cell proliferation. In incised stems of Pro_{35S}*:ANAC071-SRDX* plants, expression of *XTH20* and *XTH19* was substantially and moderately decreased, respectively. *XTH20* and *XTH19* expression and pith cell proliferation were suppressed in *anac071* plants and were increased in Pro_{35S}*:ANAC071* plants. Pith cell proliferation was also inhibited in the *xth20xth19* double mutant. Furthermore, ANAC071 bound to the *XTH20* and *XTH19* promoters to induce their expression. This is the first study revealing *XTH20* and *XTH19* induction by auxin via ANAC071 in the distal part of an incised stem and their involvement in cell proliferation in the tissue reunion process.

Key words: incision of stem, pith cell proliferation, transcription factors, *XTH*, auxin, tissue reunion

INTRODUCTION

Injuries caused by wind, herbivores, and chewing insects are one of the critical environmental factors affecting plant survival. Therefore, plants have developed primary physical barriers such as cuticle, bark, and thorns. Defense responses are activated by wound response hormones like ethylene and jasmonic acid to prevent further damage when injuries occur (León et al., 2001). Unlike other organs, stems provide essential structural support and deliver nutrients, water, and physiological and chemical information between organs through vascular tissues (Satoh, 2006; Kehr and Buhtz, 2008). Therefore, damaged stems need to be repaired as soon as possible to recover their physiological functions. This ability has long been used for agricultural grafting. The mechanism of the tissue reunion process has been explored to improve grafting efficiency and overcome tissue incompatibility. Turnbull et al. (2002) developed micro-grafting in young *Arabidopsis* seedlings to study long-distance signaling pathways including flowering, systemic acquired resistance, and abiotic stress responses. In mature *Arabidopsis*, homografts and heterografts were used as a model system to study the compatibility and ontogeny of graft union formation (Flaishman et al., 2008).

Although regeneration of vascular tissue in damaged stems has been widely observed (Flaishman et al., 2003), adherence between incised or separated tissues is also required for the tissue repair process. Auxin is required to heal the hypocotyl graft between the scion and root stock in *Arabidopsis* (Yin et al., 2012). Analysis of partially incised hypocotyls of cucumber and tomato also indicates the importance of endogenous gibberellin and Mn, Zn, and B mineral elements for repairing incised hypocotyls (Asahina

et al., 2002; Asahina et al., 2006). Microarray analysis of *Arabidopsis* inflorescence stems, which was used to better understand the molecular basis of tissue repair, showed the up-regulation of genes involved in cell division, cell wall modification, and phytohormone synthesis and signaling (Asahina et al., 2011). According to analyses of the *pin1-1* mutant, which is lacking a functional auxin efflux carrier for polar transport of auxin, and decapitated plants with or without indole acetic acid (IAA) application, auxin (i) is a key factor controlling cell division in pith tissue during the repair of incised *Arabidopsis* stems, and (ii) induces expression of *ANAC071*, a NAM, ATAF1/2, CUC2 (NAC)-type transcription factor, in the distal region of the incision (Asahina et al., 2011). Recently, the involvement of *ARF6* and *ARF8* has been clarified in auxin signaling for this process (Pitaksaringkarn et al., 2014). The NAC domain was originally characterized from consensus sequences from petunia NAM and from *Arabidopsis* ATAF1, ATAF2, and CUC2 (Olsen et al., 2005). NAC family genes are plant-specific transcription factors and are expressed in various developmental stages and tissues (Kubo et al., 2005; Mitsuda et al., 2005). The control of downstream target genes by NAC has been demonstrated in dehydration stress responses (Tran et al., 2004), secondary wall biosynthesis (Zhong et al., 2007), and defense responses in *Arabidopsis* (Bu et al., 2008)**.**

Using *Pro$_{35S}$:ANAC071-SRDX* transgenic plants, we have shown that *ANAC071* controls cell proliferation in pith tissue after an incision is made (Asahina et al., 2011). However, the control of downstream targets by *ANAC071* remains unknown. The target genes should be included in the up-regulated genes reported in our previous microarray analysis. Indeed, *XTH20* (xyloglucan endotransglucosylase/hydrolases20) was up-regulated

in the microarray analysis of the tissue reunion process (Asahina et al., 2011). The *XTH* family is implicated as having a principal role in the construction and restructuring of xyloglucan crosslinking within the cellulose/xyloglucan framework by catalyzing molecular grafting and/or hydrolysis of xyloglucans. XTHs are also involved in various physiological processes, mainly by participating in cell enlargement (Nishitani and Tominaga, 1992; Okazawa et al., 1993; Fry, 2004). *XTH20* is induced by auxin in roots (Vissenberg et al., 2005; Osato et al., 2006). Here we found that *XTH20* was also induced in decapitated plants with IAA application as well as when *ANAC071* was induced. These results suggested that *XTH20* may be a downstream target of *ANAC071* as a consequence of auxin action in incised stems. We also show the involvement of XTH in cell proliferation in plant tissue.

RESULTS

Differences in sugar composition in incised and non-incised *Arabidopsis* inflorescence stems

In our microarray analysis of *Arabidopsis* inflorescence stems, up-regulation of some enzymes for the metabolism of cell wall polysaccharides was observed (Asahina et al., 2011). The families of up-regulated genes included the enzymes that degrade cell wall polysaccharides such as polygalacturonase, pectate lyase, pectin methylesterase, glycosyl hydrolase, and β-glucosidase. In contrast, *FUT3*, a homolog of *FUT1* (xyloglucan fucosyltransferase) (Vanzin et al., 2002) was the only upregulated glycosyltransferase. To comprehensively survey cell wall polysaccharides for this study, we sequentially treated

Arabidopsis cell walls with α-amylase, endo-polygalacturonase, and Na_2CO_3 to extract the pectin fractions and then treated them with 1 M KOH and 4 M KOH to extract hemicellulose fractions; the insoluble residue was considered to be a cellulose fraction. Monosaccharide composition analysis was performed on these fractions. Differences in monosaccharide composition were present only in the pectin fractions, and the arabinose content increased in incised stems (Table S1).

Glycosyl linkage analysis was also performed on the α-amylase fraction, because this fraction contains the majority of pectic polysaccharides and because half of the cell wall pectin is released by this treatment in *Arabidopsis* (Zablackis et al., 1995). Glycosyl linkage analysis showed that terminal and 5-linked arabinofuranosyl residues increased in incised stems (Table S2). These results suggest that branched arabinan side chains of pectin increase in incised stems, because the backbones of pectic arabinans specifically consist of α-1,5-L-arabinofuranose.

Although these results showed an increase in pectin in incised stems, our previous microarray data (Asahina et al., 2011) did not show the up-regulation of the genes involved in pectin biosynthesis including the *GAUT1* (Atmodjo et al., 2011) and *ARAD1* (Harholt et al., 2006) gene families. In addition to the up-regulation of genes for the enzymes responsible for degrading cell wall polysaccharides, we did note the up-regulation of *XTH20* and *Expansin10* (Cho and Cosgrove, 2000), which are involved in the modification of the cross-link between xyloglucan and cellulose microfibril. These results indicated that the modification and reconstruction of the cell wall network might be promoted during tissue reunion.

Spatial and temporal expression of *ANAC071, XTH20,* and *XTH19* in incised *Arabidopsis* inflorescence stems

The expression levels of *ANAC071, XTH20,* and *XTH19,* which is phylogenetically closest to *XTH20,* were determined in various organs of *Arabidopsis* by quantitative RT-PCR. These genes were highly expressed in incised inflorescence stems. *XTH20* and *XTH19* were also highly expressed in roots, but the concomitant expression of *ANAC071* was observed only in incised stems (Figure 1a, 1b, and 1c). The tissue-specific expression of *ANAC071*, *XTH20*, and *XTH19* was examined in more detail using promoter-reporter markers. The 1.5-kb upstream region of each gene was fused with the β-glucuronidase (GUS) reporter gene and introduced into *Arabidopsis*. $Pro_{ANAC071}$*:GUS* was highly expressed in the distal region 1 and 3 days after the incision was made (Figure 1d and 1e), confirming our previous quantitative RT-PCR results showing that *ANAC071* is specifically expressed in the distal region of incised inflorescence stems (Asahina et al., 2011). The expression of *XTH20* and *XTH19* was higher in the distal than proximal regions of the incision at 1 day (Figure 1p, and 1q), but expression of *XTH19* was similar in both regions at 3 and 5 days (Figure 1q). In Pro_{XTH20}*:GUS* and Pro_{XTH19}*:GUS* transgenic plants, GUS activity was higher in the distal than the proximal region for Pro_{XTH20}*:GUS*, but expression was similar in both regions for Pro_{XTH19}*:GUS* (Figure 1h–1o). *XTH19* was also expressed in the siliques and flowers of intact plants (Figure 1c). These results indicated that the expression of *ANAC071* and the expression of *XTH20* are highly correlated.

Induction of *ANAC071, XTH20,* and *XTH19* by auxin in incised *Arabidopsis* inflorescence stems

Similar to previous results (Asahina et al., 2011), the expression of $Pro_{ANAC071}$*:GUS* in response to auxin was higher in the distal part of the incision. The expression of *XTH20* and *XTH19* was also induced by IAA application (Figure 2a and 2b). In Pro_{XTH20}*:GUS* transgenic plants, GUS activity was high in the distal region of the incision after IAA application, which was similar to the pattern with $Pro_{ANAC071}$*:GUS* (Figure 2d and 2f). In Pro_{XTH19}*:GUS* transgenic plants, GUS activity was detected in both the distal and proximal regions of the incision after IAA application, but the level of Pro_{XTH19}*:GUS* was higher in the distal region (Figure 2h). These results indicated that *ANAC071*, *XTH20,* and *XTH19* are auxin-inducible genes in incised *Arabidopsis* stems and that the expression of *XTH20* is more closely correlated with that of auxin-induced *ANAC071* than is *XTH19*.

Effect of gravity on tissue repair in *Arabidopsis* incised inflorescence stems

Auxin is involved in gravity responses in stems and roots, and thus the effect of the gravity response on the tissue repair process was examined. After incision of the stems, the plants were incubated in a horizontal position with the incision site facing either downward or upward, in the same or opposite direction as the gravity vector, respectively. Pith cell number 7 days after the incision was made did not increase at the cut surface for those plants grown with an upward-facing incision (Figure 3a–3d). In addition, GUS activity in $Pro_{ANAC071}$*:GUS*, Pro_{XTH20}*:GUS*, Pro_{XTH19}*:GUS*, and Pro_{DR5}*:GUS* (to monitor the auxin response) transgenic plants decreased when the incision sites were upward facing as

compared with downward-facing incisions and control (i.e. vertical) stems (Figure 3e–3p). All of these results indicated a good correlation between the auxin response and *ANAC071*, *XTH20*, and *XTH19* expression.

Control of the expression of *XTH20* and *XTH19* by *ANAC071* in incised *Arabidopsis* stems

As described above, the expression of *ANAC071*, *XTH20*, and *XTH19* was correlated with the incision response (Figure 1) and with the auxin response (Figures 2 and 3), and *ANAC071* is a key auxin-response factor that controls tissue reunion (Asahina et al., 2011). Hence, the expression levels of *XTH20* and *XTH19* were examined in incised stems of *Pro$_{35S}$:ANAC071-SRDX* transgenic plants to determine whether *XTH20* and *XTH19* are controlled by *ANAC071*. The expression level of *XTH20* in incised stems substantially decreased in *Pro$_{35S}$:ANAC071-SRDX* transgenic plants (Figure 4a). Moreover, the expression level of *XTH19* in incised stems of *Pro$_{35S}$:ANAC071-SRDX* transgenic plants decreased moderately (Figure 4b). Furthermore, decreased expression of *XTH20* and *XTH19* in the *anac071* T-DNA insertion mutant and increased expression in *Pro$_{35S}$:ANAC071* transgenic plants were observed (Figure 4c and 4d). These results indicated that *XTH20* and *XTH19* may be downstream genes under the control of *ANAC071* in incised *Arabidopsis* stems.

Binding of ANAC071 to *XTH20* and *XTH19* promoters

The *Arabidopsis* NAC protein family targets the recognition sequence CATGT and the core binding site CACG to bind with promoters of downstream genes (Bu et al., 2008). The promoters of *XTH20* and *XTH19* at –923 bp and –102 bp upstream from their respective coding sequences (Figure 5a and 5b) had sequences similar to the recognition site (CATG) and core binding site (CACC) (Figure 5c and 5d). Hence, we examined whether ANAC071 binds to the promoters of *XTH20* and *XTH19* using an electrophoretic mobility shift assay (EMSA). Purified His-ANAC071 fusion protein was incubated with labeled DNA probes, and an EMSA was performed. A high-affinity DNA-protein complex was detected (Figure 5e and 5f; lane 2 arrowhead), and DNA binding was reduced by the addition of an excess of unlabeled oligonucleotide probes corresponding to the *XTH20* or *XTH19* promoter, which acted as specific competitors (Figure 5e and 5f; lanes 3 and 4). Moreover, *Agrobacterium*-mediated transient expression of *ANAC071* driven by Pro_{35S} in the leaves of Pro_{XTH20}*:GUS* and Pro_{XTH19}*:GUS* transformants showed significantly higher GUS activity than the empty vector control (Figure S1). These results suggest that ANAC071 controls *XTH20* and *XTH19* expression by binding to their respective promoters.

ANAC071, XTH19, and *XTH20* control cell proliferation in pith tissue of incised *Arabidopsis* stems

Because *XTH20* and *XTH19* were controlled by ANAC071, the tissue reunion phenotype was examined in the *anac071* mutant and in Pro_{35S}*:ANAC071* transgenic plants, as well as in the *xth19* and *xth20* mutants 1, 3, 5, and 7 days after the incision was made (Figure 6, Figure S2, and Figure S3). The *anac071* mutant had fewer pith cells than wild type (Figure

6a, 6b, and 6i), as was previously described for *Pro$_{35S}$:ANAC071-SRDX* transgenic plants (Asahina et al., 2011). Introduction of *Pro$_{35S}$:ANAC071* into the *anac071* background restored cell division in pith tissue (Figure 6c and 6i). Moreover, two lines of *Pro$_{35S}$:ANAC071* transgenic plants showed higher cell numbers in pith tissue than in wild-type control plants (Figures 6a, 6d, 6e, and 6i) . These results suggested that *ANAC071* controls the tissue reunion process by controlling cell proliferation in the pith tissue.

To monitor the effects of *ANAC071* on auxin flow and/or responses in stems, the expression of *IAA5*, the incision-inducible auxin response gene (Asahina et al., 2011), was examined in incised and non-incised stems. *IAA5* expression decreased in the non-incised stems of *anac071* and increased in those of *Pro$_{35S}$:ANAC071* transgenic plants. In contrast, *IAA5* expression in incised stems was not substantially different among wild type, *anac071*, and *Pro$_{35S}$:ANAC071* transgenic plants (Figure S4). These results suggest that changes in auxin transport and/or responses may not be the main factor in the control of cell division by *ANAC071*.

In terms of general plant morphology, rosette leaf number, length, and width were reduced in the *anac071* mutant and slight increases in those traits were observed in *Pro$_{35S}$:ANAC071* transgenic plants (Figure S5), as was an increase in the size of mesophyll and epidermal cells in rosette leaves of *Pro$_{35S}$:ANAC071* transgenic plants (Figure S6). These results suggest that cell growth is likely to be involved in the promotion of leaf growth by *ANAC071*.

To study the function of *XTH20* in the tissue reunion process, we examined the *xth20* T-DNA insertion mutant. In the *xth20* single mutant 7 days after the incision was

made, the number of pith cells was not significantly different from wild type (Figure 6a, 6f, and 6i). We hypothesized that *XTH20* may act redundantly with *XTH19*. The single mutant of *XTH19* had similar pith cell numbers as wild-type control plants (Figure 6a, 6g, and 6i). Furthermore, we generated the *xth20xth19* mutant, which exhibited fewer pith cells 7 days after the incision was made than wild type (Figure 6h and 6i). In those incised stems 3 days after the incision was made, the expression of *CYCB1;1* was not significantly different between wild type and *xth20xth19* (Figure S7). These results support our hypothesis that *XTH20* and *XTH19* are functionally redundant and are involved in the cell proliferation of pith tissue during the tissue reunion process.

The primary root length of *xth20xth19* was significantly decreased as compared with that of *xth20*, *xth19*, and wild-type plants (*t*-test, $P < 0.05$) (Figure S8a and S8b). In addition, the lengths of meristematic zones and epidermal cells of *xth20xth19* roots were shorter than those of wild type (Figure S9a-f). These results are consistent with the finding that *XTH20* and *XTH19* were highly expressed in intact roots (Figure 1b and 1c). Because the levels of *CYCB1;1* expression were not significantly different between wild type and *xth20xth19* (Figure S10), these root-expressed *XTHs* are likely to be involved in root growth mainly via the promotion of cell growth.

DISCUSSION

Auxin is involved in the induction of *ANAC071*, *XTH20*, and *XTH19*

Auxin is produced in the apical meristem and is transported to all plant organs (Robert and Friml, 2009). Auxin plays an important role in cell proliferation and vascular differentiation (Berleth et al., 2000; Flaishman et al., 2003; Teala et al., 2006). Histochemical analysis of *Pro$_{DR5}$:GUS* transformants, which can be used to monitor auxin accumulation, showed high GUS activity in the distal region of the incision 3 days after the incision was made (Figure 3e). Tissue reunion is strongly inhibited by decapitation of or TIBA (an inhibitor of auxin polar transport) application to wild-type plants and on *pin1-1* mutants, whereas the application of 10^{-3} M IAA to decapitated plants leads to the recovery of the reunion process (Asahina et al., 2011). These results indicate that auxin is a key factor in the regulation of tissue repair in the *Arabidopsis* incised inflorescence stem. Xie et al. (2000) reported that *NAC1* is induced by auxin and promotes lateral root formation. Previous studies suggest that some *XTH* genes, including *XTH20* and *XTH19*, are regulated by auxin in the roots (Vissenberg et al., 2005; Osato et al., 2006). Application of IAA to decapitated stems increased both *XTH20* and *XTH19* expression (Figure 2a and 2b), and the direction of gravity controlled their expression (Figure 3l and 3o) as well as the expression of *ANAC071* (Figure 3i). However, *XTH19* was also expressed in the proximal region of the incision (Figure 1m and 1q, Figure 2h) and was constitutively expressed in the silique and flower (Figure 1c). Thus *ANAC071*, *XTH20*, and *XTH19* were induced by auxin in the tissue reunion process, but *XTH19* may also be controlled by other factors.

ANAC071 acts as a regulator in the tissue reunion process

The plant-specific NAC transcription factor family, with 105 members predicted in the *Arabidopsis* genome (Ooka et al., 2003), is important for various physiological processes such as lateral root formation, auxin signaling, responses to abiotic stress (Olsen et al., 2005), xylem formation (Kubo et al., 2005), and thickening of the secondary wall (Mitsuda et al., 2005). We previously reported the use of *Pro$_{35S}$:ANAC071-SDRX* to show that *ANAC071* controls the tissue reunion process in incised inflorescence stems (Asahina et al., 2011). Here we showed that the expression levels of *ANAC071* in the *anac071* mutant and in *Pro$_{35S}$:ANAC071* transgenic plants and the expression of *Pro$_{35S}$:ANAC071-SRDX* were correlated with the expression of *XTH20* and *XTH19* (Figure 4a–4d). The *anac071* mutant showed strong inhibition of the reunion process (Figure 6b and 6i). Complementation of *anac071* with *ANAC071* also showed recovery of cell proliferation in pith tissue (Figure 6c and 6i). Moreover, wild-type plants that over-expressed *ANAC071* had more cell proliferation than did wild-type control plants (Figure 6a, 6d, 6e, and 6i), but auxin flow and/or responses monitored by *IAA5* expression were not largely enhanced in *Pro$_{35S}$:ANAC071* transgenic plants (Figure S4).These results suggest that *ANAC071* is an important transcription factor that controls its downstream genes and pith cell proliferation in the tissue reunion process.

ANAC071 controls *XTH20* and *XTH19*

The expression of *XTH20* and *XTH19* in both incised and non-incised tissue decreased in *Pro$_{35S}$:ANAC071-SRDX* plants (Figure 4a and 4b). The expression of *XTH20* and *XTH19* decreased in *anac071* plants, particularly 3 days after the incision was made, but

substantially increased in *Pro$_{35S}$:ANAC071* transgenic plants (Figure 4c and 4d). These results suggested that *ANAC071* controls the expression of *XTH20* and *XTH19* in the tissue reunion process. Bu et al. (2008) demonstrated the direct binding of ANAC019 to the VSP1 promoter, which contains the recognition site (CATGT) and core binding site (CACG) for the NAC protein family. The promoters of *XTH20* and *XTH19* also contain a similar recognition site (CATGT and CATG) and core binding site (CACC), which differs from the usual core binding site (CACG) for NAC proteins (Figure 5c and 5d). EMSA assays (Figure 5e and 5f) and the promotion of the expressions of *XTH20* and *XTH19* by the transient expression of *ANAC071* (Figure S1) suggest that the ANAC071 protein binds to the promoters of *XTH20* and *XTH19* to promote their expression and that the CACC sequence is important for recognition by ANAC071. The expression pattern of *XTH20* (Figure 1i and 1p) was different from that of *XTH19* (Figure 1m and 1q), suggesting that some unknown factor(s) participates in the expression of *XTH19* in the proximal region of the incised stem.

XTH20 and *XTH19* act redundantly in the tissue reunion process

Sugar composition and sugar linkage analysis of the fractions of cell wall polysaccharides showed the increase in arabinan side chains of pectin in incised stems (Table S1 and Table S2). *ARAD1* is the only glycosyltransferase gene that is known to be involved in the synthesis of pectic arabinan (Harholt et al., 2006), but its up-regulation was not observed in the previous microarray analysis (Asahina et al., 2011). In contrast, the genes for pectin modification and degradation enzymes were up-regulated, and hence pectin turnover might

be involved in the tissue-reunion process. Although no obvious changes were observed in the composition of hemicellulosic sugars in incised stems (Table S1), remodeling of the hemicellulose network with cellulose might occur in the tissue reunion. Actually, some of the genes for altering xyloglucan-cellulose cross-linking, including *XTH20* and *Expansin10,* were noted in the previous microarray analysis (Asahina et al., 2011).

The function of XTHs is to split and reconnect xyloglucan molecules in plant cell walls, thereby affecting cell enlargement (Nishitani and Tominaga, 1992; Okazawa et al., 1993; Fry, 2004). Hyodo et al. (2003) suggested the involvement of *XTH9* in cell elongation in the flowering stem. Rose et al. (2002) revealed the gene structure and phylogenetic tree of the *Arabidopsis XTH* family, showing that *XTH20* and *XTH19* are close homologs. Vissenberg et al. (2005) reported the differential expression of *XTH17*, *XTH18, XTH19,* and *XTH20,* which have highly conserved sequences in the promoter region. In our experiment, the *xth20* single mutant did not show an inhibition of the reunion process (Figure 6f). Thus, *XTH20* may act redundantly with other genes that regulate this process. Therefore, we made a double mutant of *XTH20* and *XTH19*. *xth20xth19* showed strong inhibition of the reunion process (Figure 6h) and a lower pith cell number (Figure 5i) without changes in *CYCB1;1* expression (Figure S7). In addition, the length of primary roots**,** as well as the lengths of meristematic zones and epidermal cells, also decreased in *xth20xth19* (Figure S8a and S8b and Figure S9a-S9f) without changes in *CYCB1;1* expression (Figure S10). These results indicated that *XTH20* and *XTH19* act redundantly to control cell proliferation in the reunion process as well as primary root elongation possibly

by a mechanism that does not involve controlling the cell cycle. As far as we know, this is the first report showing that XTH is involved in cell proliferation in plant tissue.

During cytokinesis, the nascent cell wall produces a cell plate that fuses to the pre-existing cell wall of the mother cell. This process involves the restructuring of xyloglucan cross-links in the cellulose/xyloglucan framework, which could possibly include a role for XTH20 and XTH19. Yokoyama and Nishitani (2001) have also hypothesized a function for XTHs in cell plate formation during cytokinesis by showing the localization of XTH in the cell plates of BY-2 cells. During cell plate formation, xyloglucan molecules that are produced and transported from the Golgi apparatus may be required as materials for cell plates and nascent cell walls (Moore and Staehelin, 1988). Future research will elucidate how XTHs control cell proliferation and/or cytokinesis by modulating the xyloglucan molecules and the cellulose/xyloglucan framework in the cell plate and/or cell wall.

EXPERIMENTAL PROCEDURES

Plant materials and growth conditions

The *Arabidopsis* T-DNA insertion mutants *anac071* (SALK_012841), *xth20* (SALK_066758), and *xth19* (GABI Kat 369E06) were obtained from the Arabidopsis Biological Resource Center at Ohio State University (Alonso et al., 2003). The homozygous lines were selected by PCR using specific primers (Table S3), and expression levels of the relevant genes were confirmed as compared with wild-type plants (Figure S3a–S3c).

To generate the transgenic plants, the amplified fragments were cloned into pENTR/D-TOPO vector (Invitrogen; pENTR™ Direction TOPO® Cloning Kits) (Table S3). The inserts from entry clones were then integrated into binary vectors pKGWFS7 for the expression of GUS and pK2GW7 for over-expression using LR Clonase (Invitrogen), and the constructed plasmids were used for *Agrobacterium*-mediated transformation of *Arabidopsis* (Col-0) (see below). Transformants were selected by kanamycin, and the expression levels of the relevant genes were confirmed as compared with wild-type plants.

Arabidopsis seed materials were vernalized in sterilized distilled water at 4°C for 3 days and then germinated on half-strength MS medium at 22°C under continuous light conditions (32 μmol m^{-2} s^{-1}). After 3 weeks of germination, the plants were transferred to soil and grown under the same conditions until bolting.

To generate incised plants, the first internode of the inflorescence stem was incised to half of its diameter under a stereomicroscope using a microsurgery knife (Surgical Specialties Co.) and grown for an additional 7 days under conditions as described (Asahina et al., 2011).

Microscopic analysis

Incised inflorescence stem samples were immersed overnight in fixative solution (2.5% [v/v] glutaraldehyde and 1% [w/v] paraformaldehyde in 0.1 M phosphate buffer, pH 6.8–7.4). After fixation, samples were washed twice in the same buffer, dehydrated with an ethanol series, and embedded in Technovit 7100 resin (Heraeus Kulzer). Tissue sections (2.0 μm thick) were prepared using an ultra-microtome glass knife (Reichert EM-

ULTRACUT, Leica). The sections were stained with 0.1% (w/v) toluidine blue O for 10 min. The tissue reunion region was observed with a light microscope (DMRB, Leica). Cell density of the sectioned sample 7 days after the incision was made was calculated with the method shown in Figure S11.

Decapitation and application of phytohormone

For experiments requiring decapitation, after each plant bolted, the distal region of the first internode was removed, and 10^{-3} M IAA or distilled water as a mixture with lanolin (1:1, v/v) was immediately applied. The remainder of the first internode was partially incised 24 h after application as described in Asahina et al. (2011).

Histochemical staining with 5-bromo-4-chloro-3-indolyl-β-D-clucuronide (X-Glu)

Plant tissues were softened with 90% (v/v) acetone on ice for 20 min and then immersed in staining solution (100 mM phosphate buffer [pH 7], 10 mM EDTA, 1 mM $K_3Fe(CN)_6$, 1 mM $K_4Fe(CN)_6 \cdot 3H_2O$, 0.1% [w/v] Triton X-100, and 0.1 M X-Glu) under vacuum for 30 min. The plant tissue samples were then incubated at 37°C for 8 h (Jefferson, 1987) and cleared with 70% (v/v) ethanol for ~12 h. Expression positions were observed using a stereomicroscope (Leica MCSLIII).

RNA preparation and quantitative RT-PCR

Total RNA was extracted from *Arabidopsis* incised and non-incised flowering stems with a RNAqueous RNA isolation kit with plant RNA Isolation aid (Ambion). Complementary

DNA was synthesized from total RNA (50 μg) by the QuantiTect Reverse Transcription Kit (Qiagen). Real-time PCR using TaqMan technology or SYBR Green I reagents (Qiagen) was performed using cDNA as a template on a sequence detector system (model 7000; Applied Biosystems) with specific primers (Table S3). To normalize and confirm expression levels across various stages of incision treatment, *ACT7* was used as an internal standard with three biological replications per sample.

EMSA

The coding region of *ANAC071* was amplified by PCR using specific primers (*Eco*RI sense and *Sal*I antisense; Table S3). The PCR product was digested with *Eco*RI and *Sal*I and introduced into *Eco*RI- and *Sal*I-digested pCold ProS2 (Takara). The His-Tag fusion protein was produced in *E. coli* (Origami (DE3); Novagen) and purified using His-Accept resin (Nacalai Tesque Inc.). Oligonucleotides (see primer sequences in Figure 5c and 5d) were labeled with biotin using Biotin 3' End DNA Labeling Kit (Thermo Fisher Scientific). To make double-stranded biotin-labeled probes, the complementary oligonucleotide pairs were annealed at 95°C for 5 min and slowly cooled to room temperature overnight. Double-stranded unlabeled oligonucleotides were made using the same method. The labeled probes were incubated for 1 h at 28°C with 2 μg of purified His-ANAC071 protein using the Light Shift Chemiluminescent EMSA Kit (Thermo Fisher Scientific) and were supplemented with 25 μg/mL poly (dI-dC), 0.1 μg/mL BSA, 2 mM EDTA, and 1% (w/v) NP-40. The protein-probe mixtures were separated in 6% (w/v) polyacrylamide native gels in 0.5× TBE buffer and transferred to Biodyne membrane (PALL Gelman Laboratory). Migration of the

biotin-labeled probes was visualized with the Chemiluminescent Nucleic Acid Kit (Thermo Fisher Scientific) and a detection module (LAS-4000 mini biomolecular imager; Fujifilm).

Agrobacterium-mediated transient expression

Agrobacterium tumefaciens harboring binary vector pK2GW7 with or without insertion of the full-length coding region of *ANAC071* were transformed with pCAMBIA containing *Pro$_{35S}$:Luciferase* and selected on LB plates containing kanamycin and spectinomycin. *Agrobacterium* cells were suspended in the infiltration buffer (10 mM $MgCl_2$, 10 mM MES, and 150 mM acetosyringone) at 0.5 OD_{600} and infiltrated into *Pro$_{XTH20}$:GUS* and *Pro$_{XTH19}$:GUS* transgenic plants by the leaf disc method. After 3 days of infiltration, the leaves were harvested and kept at –80°C until measurement.

Luciferase activity was measured by using a luciferase assay system (Promega, E1500), and relative light unit (RLU) was measured with a single-tube luminometer (MICROTEC, GL-200). β-glucuronidase (GUS) activity was measured with *p*-nitrophenyl-β-D-glucuronide (PNPG) as a substrate. Briefly, cell lysates were suspended to 20 mM phosphate buffer (pH 7.4) and 10 mM β-mercaptoethanol. PNPG was added to a final concentration of 1 mM, and the absorbance at 405 nm was continuously monitored.

Cell wall preparation and extraction of cell wall polysaccharides

Incised or non-incised stem segments (4 mm in length) sampled 7 days after the incision was made were individually frozen in liquid nitrogen. The material was milled using rapid

shaking twice for 30 s in a bead mill (Retsch MM400 Retsch Co., Ltd.). The material was incubated in 96% ethanol for 30 min at 70°C to inactivate enzymes. Alcohol-insoluble residues were prepared by washing the material sequentially in 100% ethanol, chloroform/methanol (1:1) twice, 65% ethanol, 80% ethanol, 100% ethanol, and finally in 100% acetone (all v/v), and air-dried. Each step was followed by centrifugation. Starch was removed by digestion with α-amylase from porcine pancreas (Type 1-A, Sigma-Aldrich; 50 U 100 mg^{-1} cell-wall materials, in 50 mM potassium phosphate buffer [pH 7.0]) overnight at 37°C with constant shaking as described by Zablackis et al. (1995). After treatment with α-amylase, the walls were treated with endo-polygalacturonase (Megazyme) as described by Ishii et al. (2001). The walls were then extracted with Na_2CO_3 as described by Selvendran and O'Neill (1987). Na_2CO_3-extracted residues were treated sequentially with 1 M KOH and 4 M KOH to solubilize hemicelluloses (Selvendran and O'Neill, 1987).

Analytical methods

Total sugar and uronic acid were determined by the phenol-sulfuric acid method (Dubois et al., 1956) with glucose as the standard and by the carbazole method (Galambos, 1967) with galacturonic acid as the standard, respectively. Neutral glycosyl-residue compositions were determined by GLC of their alditol acetate derivatives (York et al. 1985). Glycosyl-linkage compositions were determined by a modified Hakomori procedure (York et. al, 1985). Briefly, methylated polysaccharides were carboxyl reduced with Superdeuteride (1 M lithium triethylborodeuteride in tetrahydrofuran, Aldrich) as described by York et al. (1985).

The glycosyl-linkage composition was then determined by GC-MS of the partially methylated, partially acetylated alditol acetate derivatives (York et. al, 1985).

ACKNOWLEDGMENTS

Special thanks to Dr. Nobutaka Mitsuda and Dr. Masaru Ohme-Takagi of the National Institute of Advanced Industrial Science and Technology for providing *ANAC071-SRDX* transgenic *Arabidopsis* and Mr. Takashi Yamazaki, Mr. Katsuya Azuma, and Mrs. Rieko Nozawa for technical assistance. This work was supported in part by a Grant-in-Aid for Scientific Research on Priority Areas (21027004) and on Innovative Areas (24114006) to S.S.

SUPPLEMENTARY MATERIAL

The following materials are available in the online version of this article.

Figure S1. Effects of transient expression of *ANAC071* on the expression of *XTH20* and *XTH19* in the leaves of Pro_{XTH20}*:GUS* and Pro_{XTH19}*:GUS* transgenic plants.

Figure S2. Tissue reunion phenotypes at 1, 3, and 5 days after the incision was made.

Figure S3. Expression level of *ANAC071*, *XTH20*, and *XTH19*.

Figure S4. Expression of *IAA5* in incised and non-incised stems of wild type, *anac071*, and Pro_{35S}*:ANAC071* transgenic plants.

Figure S5. Morphology of plants.

Figure S6. Mesophyll and epidermal cells of wild-type, *anac071*, and *Pro35S:ANAC071* transgenic plants.

Figure S7. Expressions of *CYCB1;1* in incised and non-incised stems of wild type and *xth20xth19*.

Figure S8. Primary root length of the XTH mutants.

Figure S9. Meristematic zone and epidermal cells of wild-type and *xth20xth19* roots.

Figure S10. Expression of *CYCB1;1*, *XTH20*, and *XTH19* in roots of wild type and *xth20xth19*.

Figure S11. Method for cell density calculation.

Table S1. Monosaccharide composition in incised and non-incised inflorescence stems.

Table S2. Glycosyl-linkage composition of polysaccharides in α-amylase fraction.

Table S3. Primers used in this research.

REFERENCES

Alonso, J.M., Stepanova, A.N., Leisse, T.J., Kim, C.J., Chen, H., Shinn, P., Stevenson, D.K., Zimmerman, J., Barajas, P., Cheuk, R., Gadrinab, C., Heller, C., Jeske, A.,

Koesema, E., Meyers, C.C., Parker, H., Prednis, L., Ansari, Y., Choy, N., Deen, H., Geralt, M., Hazari, N., Hom, E., Karnes, M., Mulholland, C., Ndubaku, R., Schmidt, I., Guzman, P., Aguilar-Henonin, L., Schmid, M., Weigel, D., Carter, D.E., Marchand, T., Risseeuw, E., Brogden, D., Zeko, A., Crosby, W.L., Berry, C.C., and Ecker, J.R. (2003) Genome-wide insertional mutagenesis of *Arabidopsis thaliana. Science*, **301**, 653–657.

Asahina, M., Azuma, K., Pitaksaringkarn, W., Yamazaki, T., Mitsuda, N., Ohme-Takagi, M., Yamaguchi, S., Kamiya, Y., Okada, K., Nishimura, T., Koshiba, T., Yokota, T., Kamada, H., and Satoh, S. (2011) Spatially selective hormonal control of RAP2.6L and ANAC071 transcription factors involved in tissue reunion in *Arabidopsis*. *Proc. Natl. Acad. Sci. USA*, **108**, 16128–16132.

Asahina, M., Iwai, H., Kikuchi, A., Yamaguchi, S., Kamiya, Y., Kamada, H., and Satoh, S. (2002) Gibberellin produced in the cotyledon is required for cell division during tissue reunion in the cortex of cut cucumber and tomato hypocotyls. *Plant Physiol*., **129**, 201–210.

Asahina, M., Gocho, Y., Kamada, H., and Satoh, S. (2006) Involvement of inorganic elements in tissue reunion in the hypocotyl cortex of *Cucumis sativus*. *J. Plant Res*., **119**, 337–342.

Atmodjo, M. A., Sakuragi, Y., Zhua, X., Burrell, A. J., Mohanty, Atwood III, S. S., Orlando, R., Scheller, H. V. and Mohnen, D., (2011**)** Galacturonosyltransferase (GAUT)1 and GAUT7 are the core of a plant cell wall pectin biosynthetic

homogalacturonan:galacturonosyltransferase complex. *Proc. Natl. Acad. Sci. USA*, **108**, 20225–20230.

Berleth, T., Mattsson, J., and Hardtke, C.S. (2000) Vascular continuity and auxin signals. *Trends Plant Sci*., **5**, 387–393.

Bu, Q., Jiang, H., Li, C.-B., Zhai, Q., Zhang, J., Wu, X., Sun, J., Xie, Q., and Li, C. (2008) Role of the *Arabidopsis thaliana* NAC transcription factors ANAC019 and ANAC055 in regulating jasmonic acid-signaled defense responses. *Cell Res*., **18**, 756–767.

Cho, H.-T., and Cosgrove, D. J. (2000) Altered expression of expansin modulates leaf growth and pedicel abscission in *Arabidopsis thaliana*. *Proc. Natl. Acad. Sci. USA*, **97**, 9783–9788.

Dubois, M., Gilles, K.A., Hamilton, J.K., Rebers, P.A., and Smith, F. (1956) Colorimetric method for determination of sugars and related substances. *Anal Chem*., **28**, 350-356.

Flaishman, M. a., Loginovsky, K., Golobowich, S., and Lev-Yadun, S. (2008) *Arabidopsis thaliana* as a model system for graft union development in homografts and heterografts. *J. Plant growth regul.*, **27**, 231–239.

Flaishman, M. a., Loginovsky, K., and Lev-Yadun, S. (2003) Regenerative xylem in inflorescence stems of *Arabidopsis thaliana*. *J. Plant Growth Regul*., **22**, 253–258.

Fry, S.C. (2004). Primary cell wall metabolism : tracking the careers of wall polymers in living plant cells. *New Phytol*., **161**, 641–675.

Fukaki, H., Fujisawa, H., and Tasaka, M. (1996) Gravitropic response of inflorescence stems in *Arabidopsis thaliana*. *Plant Physiol*., **110**, 933–943.

Galambos, J.T. (1967) The reaction of carbazole with carbohydrates. I. Effect of borate and sulfamate on the carbazole color of sugars. *Anal Biochem*., **19**, 119–132.

Harholt, J., Jensen, J.K., Sørensen, S.O., Orfila, C., Pauly, M. and Scheller, H.V. (2006**)** ARABINAN DEFICIENT 1 is a putative arabinosyltransferase involved in biosynthesis of pectic arabinan in Arabidopsis. *Plant Physiol.*, **140**, 49-58.

Hyodo, H., Yamakawa, S., Takeda, Y., Tsuduki, M., Yokota, A., Nishitani, K., and Kohchi, T. (2003) Active gene expression of a xyloglucan endotransglucosylase/hydrolase gene, XTH9, in inflorescence apices is related to cell elongation in *Arabidopsis thaliana*. *Plant Mol. Biol*., **52**, 473–482.

Ishii, T., Matsunaga, T. and Hayashi, N. (2001) Formation of rhamnogalacturonan II-borate dimer in pectin determines cell wall thickness of pumpkin tissue. *Plant Physiol*., **126**, 1698-1705.

Jefferson, R.A. (1987) Assaying chimeric genes in plants: The GUS gene fusion system**.** *Plant Mol. Biol.*, **5**, 387–405.

Kehr, J. and Buhtz, A. (2008) Long distance transport and movement of RNA through the phloem. *J. Exp. Bot*., **59**, 85–92.

Kubo, M., Udagawa, M., Nishikubo, N., Horiguchi, G., Yamaguchi, M., Ito, J., Mimura, T., Fukuda, H., and Demura, T. (2005) Transcription switches for protoxylem and metaxylem vessel formation. *Genes Dev*., **19**, 1855–1860.

Tran, L.P., Nakashima, K., Sakuma, Y., Simpson, S.D., Fujita, Y., Maruyama, K., Fujita, M., Seki, M., Shinozaki, K., and Yamaguchi-shinozaki, K. (2004) Isolation and Functional Analysis of Arabidopsis Stress-Inducible NAC Transcription Factors That Bind

to a Drought-Responsive cis-Element in the *early responsive to dehydration stress* 1 Promoter. *Plant cell*, **16**, 2481–2498.

León, J., Rojo, E., and Sánchez-Serrano, J.J. (2001) Wound signalling in plants. *J. Exp. Bot.*, **52**, 1–9.

Mitsuda, N., Seki, M., Shinozaki, K., and Ohme-takagi, M. (2005) The NAC transcription factors NST1 and NST2 of *Arabidopsis* regulate secondary wall thickenings and are required for anther dehiscence. *Plant Cell*, **17**, 2993–3006.

Moore, P.J. and Staehelin, L.A. (1988) Immunogold localization of the cell-wall-matrix polysaccharides rhamnogalacturonan I and xyloglucan during cell expansion and cytokinesis in Trifolium pratense L .; implication for secretory pathways. *Planta*, **174**, 433–445.

Nishitani, K. and Tominaga, R. (1992) Endo-xyloglucan transferase, a novel class of glycosyltransferase that catalyzes transfer of a segment of xyloglucan molecule to another xyloglucan molecule. *J. Biol. Chem.*, **267**, 21058–21064.

Okazawa, K., Sato, Y., Nakagawa, T., Asada, K., Kato, I., Tomita, E., and Nishitani, K. (1993) Molecular cloning and cDNA sequencing of endoxyloglucan transferase, a novel class of glycosyltransferase that mediates molecular grafting between matrix polysaccharides in plant cell walls. *J. Biol. Chem.*, **268**, 25364–25368.

Olsen, A.N., Ernst, H. a, Leggio, L. Lo, and Skriver, K. (2005) NAC transcription factors: structurally distinct, functionally diverse. *Trends Plant Sci.*, **10**, 79–87.

Ooka, H., Satoh, K., Doi, K., Nagata, T., Otomo, Y., Murakami, K., Matsubara, K., Osato, N., Kawai, J., Carninci, P., Hayashizaki, Y., Suzuki, K., Kojima, K., Takahara,

Y., Yamamoto, K., and Kikuchi, S. (2003) Comprehensive analysis of NAC family genes in *Oryza sativa* and *Arabidopsis thaliana*. *DNA Res*., **247**, 239–247.

Osato, Y., Yokoyama, R., and Nishitani, K. (2006) A principal role for AtXTH18 in Arabidopsis thaliana root growth: a functional analysis using RNAi plants. *J. Plant Res*., **119**, 153–162.

Pitaksaringkarn, W., Ishiguro, S., Asahina, M. and Satoh, S. (2014) *ARF6* and *ARF8* contribute to tissue reunion in incised *Arabidopsis* inflorescence stems. *Plant Biotechnol*., **31**, 49-53.

Robert, H.S. and Friml, J. (2009) Auxin and other signals on the move in plants. *Nature Chem Biol*., **5**, 325–332.

Rose, J.K.C., Braam, J., Fry, S.C., and Nishitani, K. (2002) The XTH family of enzymes involved in xyloglucan endotransglucosylation and endohydrolysis: current perspectives and a new unifying nomenclature. *Plant Cell Physiol*., **43**, 1421–1435.

Satoh, S. (2006) Organic substances in xylem sap delivered to above-ground organs by the roots. *J. Plant Res*., **119**, 179–187.

Selvendran, R.R. and O'Neill, M.A. (1987) Isolation and analysis of cell walls from plant material. *Methods Biochem Anal*., **32**, 25-153.

Teale, W.D., Paponov, I. a, and Palme, K. (2006) Auxin in action: signalling, transport and the control of plant growth and development. *Nat. Rev. Mol. Cell Biol*., **7**, 847–859.

Turnbull, C.G.N., Booker, J.P., and Leyser, H.M.O. (2002) Micrografting techniques for testing long-distance signalling in Arabidopsis. *Plant J*., **32**, 255–262.

Vanzin, G. F., Madson, M., Carpita, N. C., Raikhel, N. V., Keegstra, K. and Reiter, W.-D. (2002**)** The *mur2* mutant of *Arabidopsis thaliana* lacks fucosylated xyloglucan because of a lesion in fucosyltransferase AtFUT1. *Proc. Natl. Acad. Sci. USA*, **99**, 3340–3345.

Xie, Q., Frugis, G., Colgan, D., and Chua, NH., (2000) Arabidopsis NAC1 transduces auxin signal downstream of TIR1 to promote lateral root development. *Genes Dev*., **14**, 3024–3036.

Vissenberg, K., Oyama, M., Osato, Y., Yokoyama, R., Verbelen, J.-P., and Nishitani, K. (2005) Differential expression of AtXTH17, AtXTH18, AtXTH19 and AtXTH20 genes in Arabidopsis roots. Physiological roles in specification in cell wall construction. *Plant Cell Physiol*., **46**, 192–200.

Yin, H., Yan, B., Sun, J., Jia, P., Zhang, Z., Yan, X., Chai, J., Ren, Z., and Zheng, G. (2012) Graft-union development : a delicate process that involves cell – cell communication between scion and stock for local auxin accumulation. *J. Exp. Bot*., **63**, 4219–4232.

Yokoyama, R. and Nishitani, K. (2001) Endoxyloglucan transferase is localized both in the cell plate and in the secretory pathway destined for the apoplast in tobacco cells. *Plant Cell Physiol*., **42**, 292–300.

York, W.S., Darvill, A.G., McNeil, M., Stevenson, T.T. and Albersheim, P. (1985) Isolation and characterization of plant cell walls and cell wall constituents. *Methods Enzymol*., **118**, 3-40. **Zablackis, E., Hunang, J., Müller, B., Darvill, A.G. and Albersheim, P.** (1995) Characterization of the cell-wall polysaccharides of *Arabidopsis thaliana* leaves. *Plant Physiol*., **107**:1129-1138.

Zhong, R., Richardson, E. a, and Ye, Z.-H. (2007) The MYB46 transcription factor is a direct target of SND1 and regulates secondary wall biosynthesis in Arabidopsis. *Plant cell*, **19**, 2776–2792.

FIGURE LEGENDS

Figure 1. Tissue-specific expression of *ANAC071*, *XTH20*, and *XTH19*.

(a–c) The expression of *ANAC071* (a), *XTH20* (b), and *XTH19* (c) was examined by quantitative RT-PCR in roots, rosette leaves, cauline leaves, incised and non-incised inflorescence stems, siliques, and flowers in wild-type plants. *Actin7* was used as an internal control.

(d–o) Promoter activity of *ANAC071*, *XTH20*, and *XTH19*. GUS activities were detected in incised inflorescence stems of $Pro_{ANAC071}$*:GUS*, Pro_{XTH20}*:GUS*, and Pro_{XTH19}*:GUS* transgenic plants. The photographs were taken 1 day (d, h, and l), 3 days (e, i, and m), 5 days (f, j, and n), and 7 days (g, k, and o) after the incision was made (indicated by arrowhead). Bar = 0.5 mm.

(p,q) The expression of *XTH20* (p) and *XTH19* (q) in non-incised and distal and proximal regions of incised inflorescence stems at 1, 3, and 5 days after the incision was made. Mean ± SD (n = 3).

Figure 2. Effect of auxin on the induction of *ANAC071*, *XTH20*, and *XTH19* in the tissue reunion process.

(a,b) Expression levels of *XTH20* (a) and *XTH19* (b) in incised (black bar) and non-incised (gray bar) stems. The expression levels of *XTH20* and *XTH19* were examined by quantitative RT-PCR in non-decapitated plants and in decapitated plants 1 day after the incision was made after decapitation followed by the application of distilled water (D.W.) or 10^{-3} M IAA at the top of the cut stems. Mean ± SD (n = 3).

(c–h) Promoter activity of *ANAC071*, *XTH20*, and *XTH19*. GUS activity was detected 1 day after an incision was made in inflorescence stems of $Pro_{ANAC071}$*:GUS*, Pro_{XTH20}*:GUS*, and Pro_{XTH19}*:GUS* transgenic plants after decapitation followed by application of distilled water (D.W.) (c, e, and g) or 10^{-3} M IAA (d, f, and h). Bar = 0.5 mm.

Figure 3. Effects of gravity on the tissue reunion process.

(a–c) Tissue reunion phenotypes observed 7 days after an incision was made in plants grown vertically (a) or horizontally with upward-facing (b) and downward-facing (c) incisions. Arrowheads indicate the position of the incision. g, gravity; pi, pith; co, cortex; vb, vascular bundle. Bar = 100 μm.

(d) Cell density in pith tissues calculated from sectioned samples as grown in (a–c). Mean ± SD (n = 7). *P < 0.05 (t-test). Calculation is described in Figure S5.

(e–p) Promoter activity of *DR5*, *ANAC071*, *XTH20*, and *XTH19*. GUS activity was detected in incised inflorescence stems of Pro_{DR5}*:GUS*, $Pro_{ANAC071}$*:GUS*, Pro_{XTH20}*:GUS*, and Pro_{XTH19}*:GUS* transgenic plants 3 days after an incision was made. Immediately after the incision was made, plants were oriented vertically as a control (e, h, k, and n) or

horizontally with upward-facing (f, i, l, and o) or downward-facing (g, j, m, and p) incisions. Bar = 0.5 mm.

Figure 4. Control of the expression of *XTH20* and *XTH19* by *ANAC071* during the tissue reunion process.

(a,b) Expression of *XTH20* (a) and *XTH19* (b) was examined by quantitative RT-PCR in inflorescence stems of wild-type (incised = blue; non-incised = red) and *Pro$_{35S}$:ANAC071-SRDX* transgenic (incised = green; non-incised = purple) plants 0–7 days after the incision was made. Mean ± SD (n = 3).

(c,d) Quantitative RT-PCR analysis of *XTH20* (c) and *XTH19* (d) in incised (black bar) and non-incised (gray bar) inflorescence stems of wild-type, *anc071*, and *Pro$_{35S}$:ANAC071* transgenic plants 3 days after the incision was made. Mean ± SD (n = 3).

Figure 5. Binding of ANAC071 to *XTH20* and *XTH19* promoters.

(a,b) Illustration of selected oligonucleotides containing the *cis*-elements of the NAC recognition site (CATGT and CATG) and a presumed core binding site (CACC) in the promoters of *XTH20* (a) (–923 bp) and *XTH19* (b) (–102 bp). Black boxes indicate exons.

(c,d) Oligonucleotides used in the EMSA. The probes for *XTH20* (c) and *XTH19* (d) (pXTH20 and pXTH19, respectively) contained the *cis*-element of the NAC recognition site (CATGT and CATG) and the presumed core binding site (CACC) in the *XTH20* and *XTH19* promoter regions.

(e,f) The EMSA showed binding of His-ANAC071 to the CATGT, CACC, and CATG motifs in *XTH20* (e) and *XTH19* (f) promoters. Protein-DNA complexes were detected when His-ANAC071 fusion protein was incubated with labeled pXTH20 or pXTH19 probes (lane 2). Unlabeled pXTH20 or pXTH19 (lanes 3 and 4) were used for 100-fold (lanes 3) and 200-fold (lanes 4) excess levels of competitors. Arrowheads indicate the position of the protein-DNA complex.

Figure 6. Phenotypes of *anac071*, *xth20*, and *xth19* single mutants and the *xth20xth19* double mutant and the effect of *ANAC071* overexpression on cell division in pith tissue.
(a–h) Tissue reunion phenotype observed 7 days after the incision was made. *Pro$_{35S}$:ANAC071* was introduced into *anac071* mutant (*Pro$_{35S}$:ANAC071* (*anac071*)) or two wild-type lines (*Pro$_{35S}$:ANAC071* #2-3 and #4-1). Arrowheads indicate the position of the incision. pi, pith; co, cortex; vb, vascular bundle; WT, wild type. Bar = 100 μm.
(i) Cell density in pith tissue was calculated from sectioned samples. Mean ± SD (n = 7). *P < 0.05 (t-test compared with WT).

SUPPLEMENTAL INFORMATION

Figure S1. Effects of transient expression of *ANAC071* on the expression of *XTH20* and *XTH19* in the leaves of *Pro$_{XTH20}$:GUS* and *Pro$_{XTH19}$:GUS* transgenic plants.

(a,b) GUS activity after infiltration of *Agrobacterium* harboring pK2GW7 containing *Pro$_{35S}$:ANAC071* or empty pK2GW7 vector and pCAMBIA containing *Pro$_{35S}$:Luciferase* (internal control) into *Pro$_{XTH20}$:GUS* (a) or *Pro$_{XTH19}$:GUS* (b) transgenic plants. Mean ± SD (n = 10). GUS activity and the relative light unit (RLU) for luciferase activity were measured 3 days after infiltration. Asterisks indicate statistically significant differences between *Pro$_{35S}$:ANAC071* and empty vector (Student's *t*-test, $P < 0.05$).

Figure S2. Tissue reunion phenotypes at 1, 3, and 5 days after the incision was made.
(a–x) Tissue reunion phenotype of wild type (a, i, q), *anac071* (b, j, r), *Pro$_{35S}$:ANAC071* in the *anac071* background (c, k, s), *Pro$_{35S}$:ANAC071* transgenic lines #2-3 (d, l, t) and #4-1 (e, m, u), *xth20* (f, n, v) and *xth19* (g, o, w) single mutants, and the *xth20xth19* double mutant (h, p, x) 1 day (a–h), 3 days (i–p), and 5 days (q–x) after the incision was made. Arrowheads indicate positions of the incision. pi, pith; co, cortex; vb, vascular bundle. Bar = 100 μm. Three plants for each genotype were examined, and representative photographs are shown.

Figure S3. Expression level of *ANAC071*, *XTH20*, and *XTH19*.
(a–c) Expression level of *ANAC071* (a), *XTH20* (b), and *XTH19* (c) in *anac071*, *Pro$_{35S}$:ANAC071* in the *anac071* background, *Pro$_{35S}$:ANAC071* transgenic lines (#2-3 and #4-1), *xth20* and *xth19* single mutants, and the *xth20xth19* double mutant as compared with wild-type plants. WT, wild type.

Figure S4. Expression of *IAA5* in incised and non-incised stems of wild-type, *anac071*, and *Pro$_{35S}$:ANAC071* transgenic plants.

Expression levels of *IAA5* in incised (black bar) and non-incised (gray bar) stems 1 day after the incision was made. Mean ± SD (n = 3). WT, wild type.

Figure S5. Morphology of plants.

(a) Photograph of wild-type, *anac071*, *Pro$_{35S}$:ANAC071* transgenic wild-type lines (#2-3 and #4-1), *Pro$_{35S}$:ANAC071* in the *anac071* background, *xth20* and *xth19* single mutants, and the *xth20xth19* double mutant (from left to right). Bar = 5 cm.

(b) Rosette leaf number in mature plants (3 weeks after transfer to soil). Mean ± SD (n = 12).

(c) Leaf length (black bar) and width (gray bar) of the sixth rosette leaf. Mean ± SD (n = 12). WT, wild type.

Figure S6. Mesophyll and epidermal cells of wild-type, *anac071*, and *Pro35S:ANAC071* transgenic plants.

(a,c,e,g) Mesophyll cells of wild type (a), *anac071* (c), *Pro35S:ANAC071* transgenic line #2-3 (e), and *Pro35S:ANAC071* transgenic line #4-1 (g). Bar = 100 μm.

(b,d,f,h) Epidermal cells of wild type (b), *anac071* (d), *Pro35S:ANAC071* transgenic line #2-3 (f), and *Pro35S:ANAC071* transgenic line #4-1 (h). Bar = 100 μm. WT, wild type.

Figure S7. Expression of *CYCB1;1* in incised and non-incised stems of wild type and *xth20xth19*.

Expression levels of *CYCB1;1* in incised (black bar) and non-incised (gray bar) stems 3 days after the incision was made. Mean ± SD (n = 3). WT, wild type.

Figure S8. Primary root length of the XTH mutants.

(a) Photograph of wild-type and XTH mutant roots 10 days after sowing plants in half-strength MS medium. Arrowheads indicate root tips.

(b) Primary root length of wild-type (white circle), *xth19* (white diamond), *xth20* (black square), and *xth20xth19* (black diamond) plants 5, 10, and 15 days after sowing. Mean ± SD (n = 12). WT, wild type.

Figure S9. Meristematic zone and epidermal cells of wild-type and *xth20xth19* roots.

(a–d) Meristematic zone (a,b) and epidermal cells (c,d) of roots of wild type (a,c) and *xth20xth19* (b,d) 10 days after sowing. Bar = 200 μm (a,b) and 100 μm (c,d). Roots were stained with 10 mg/mL propidium iodide for 5 min and observed with a confocal laser-scanning microscope (LSM 710; Carl Zeiss, Germany).

(e,f) Meristematic zone length (e) and epidermal cell length (f) of roots of wild type and *xth20xth19* 10 days after sowing. Mean ± SD (n = 8). Asterisks indicate statistically significant differences between *xth20xth19* and wild type (Student's t-test, $P < 0.05$). WT, wild type.

Figure S10. Expression of *CYCB1;1*, *XTH20*, and *XTH19* in roots of wild type and *xth20xth19*.

(a–c) Expression level of *CYCB1;1* (a), *XTH20* (b), and *XTH19* (c) of wild-type and *xth20xth19* roots 10 days after sowing. Mean ± SD (n = 3).

Figure S11. Method for cell density calculation.

(a) Selected rectangle of pith tissue around the incision site for cell counting, with width (between vascular bundles) and height (width × 2). Bar = 100 μm.

(b) The selected area was measured with ImageJ software.

(c) Average cell number was counted manually based on the formula shown. The partial cells refer to those that were touching an edge of the rectangle.

Table S1 Monosaccharide composition in incised and non-incised inflorescence stems.

Neutral monosaccharide composition of incised or non-incised *Arabidopsis* stem segments (4 mm in length) sampled 7 days after the incision was made were analyzed by gas chromatography in cell wall polysaccharide fractions. Values are the mean ± SD from three biological samples. Asterisks indicate statistically significant differences between non-incised and incised stems (Student's t-test, $P < 0.05$). ND: not detected.

Table S2 Glycosyl-linkage composition of polysaccharides in the α-amylase fraction.

Glycosyl-linkage composition of polysaccharides in the α-amylase fraction of incised or non-incised *Arabidopsis* stem segments (4 mm in length) sampled 7 days after the incision

was made were analyzed by gas chromatography–mass spectrometry. Values are the mean ± SD from three measurements. Asterisks indicate statistically significant differences between non-incised and incised stems (Student's *t*-test, $P < 0.05$).

Table S3 Primers used in this research

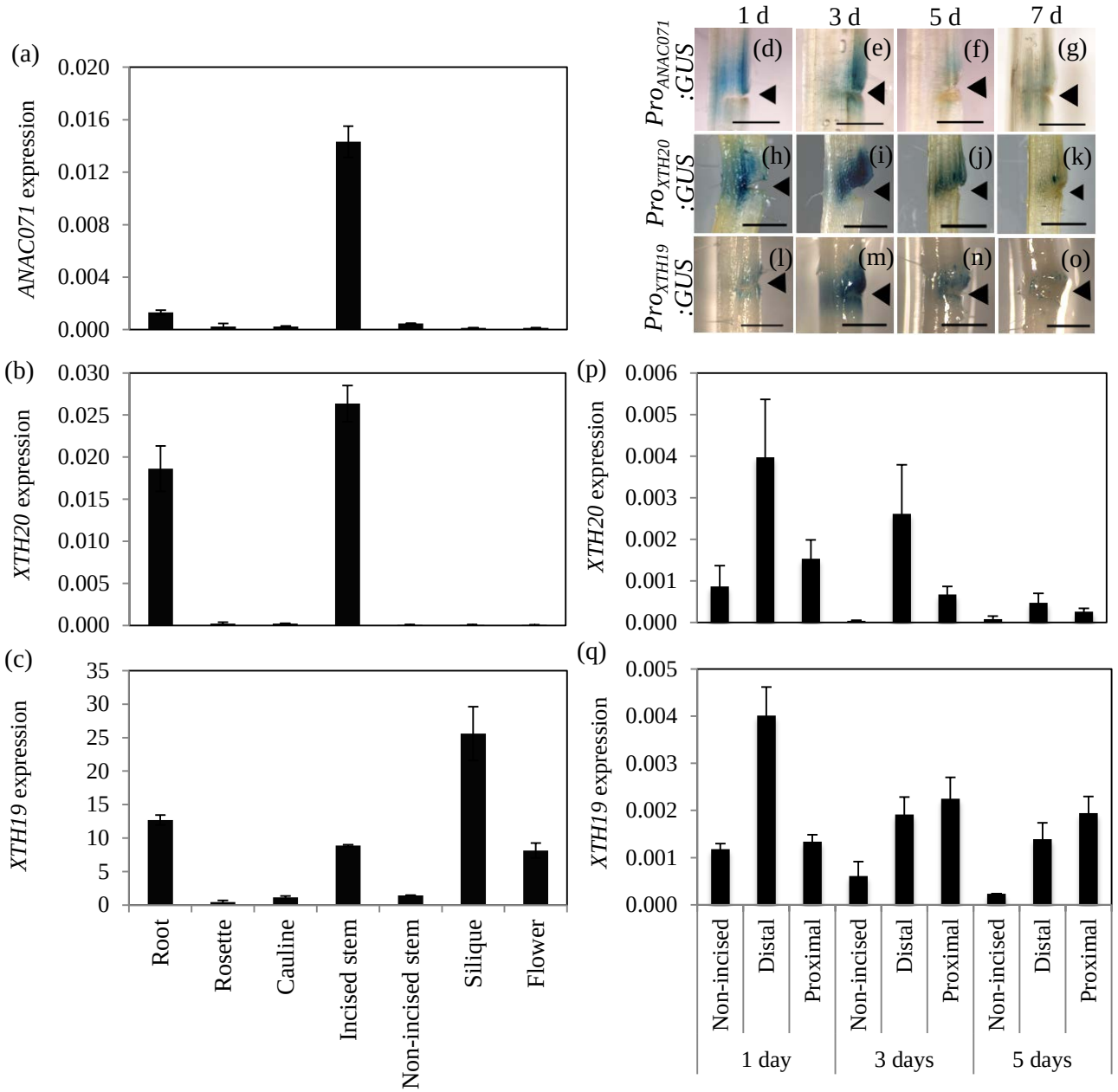

Figure 1. Tissue-specific expression of *ANAC071*, *XTH20*, and *XTH19*.

(a–c) The expression of *ANAC071* (a), *XTH20* (b), and *XTH19* (c) was examined by quantitative RT-PCR in roots, rosette leaves, cauline leaves, incised and non-incised inflorescence stems, siliques, and flowers in wild-type plants. *Actin7* was used as an internal control.

(d–o) Promoter activity of *ANAC071*, *XTH20*, and *XTH19*. GUS activities were detected in incised inflorescence stems of $Pro_{ANAC071}$*:GUS*, Pro_{XTH20}*:GUS*, and Pro_{XTH19}*:GUS* transgenic plants. The photographs were taken 1 day (d, h, and l), 3 days (e, i, and m), 5 days (f, j, and n), and 7 days (g, k, and o) after the incision was made (indicated by arrowhead). Bar = 0.5 mm.

(p,q) The expression of *XTH20* (p) and *XTH19* (q) in non-incised and distal and proximal regions of incised inflorescence stems at 1, 3, and 5 days after the incision was made. Mean ± SD (*n* = 3).

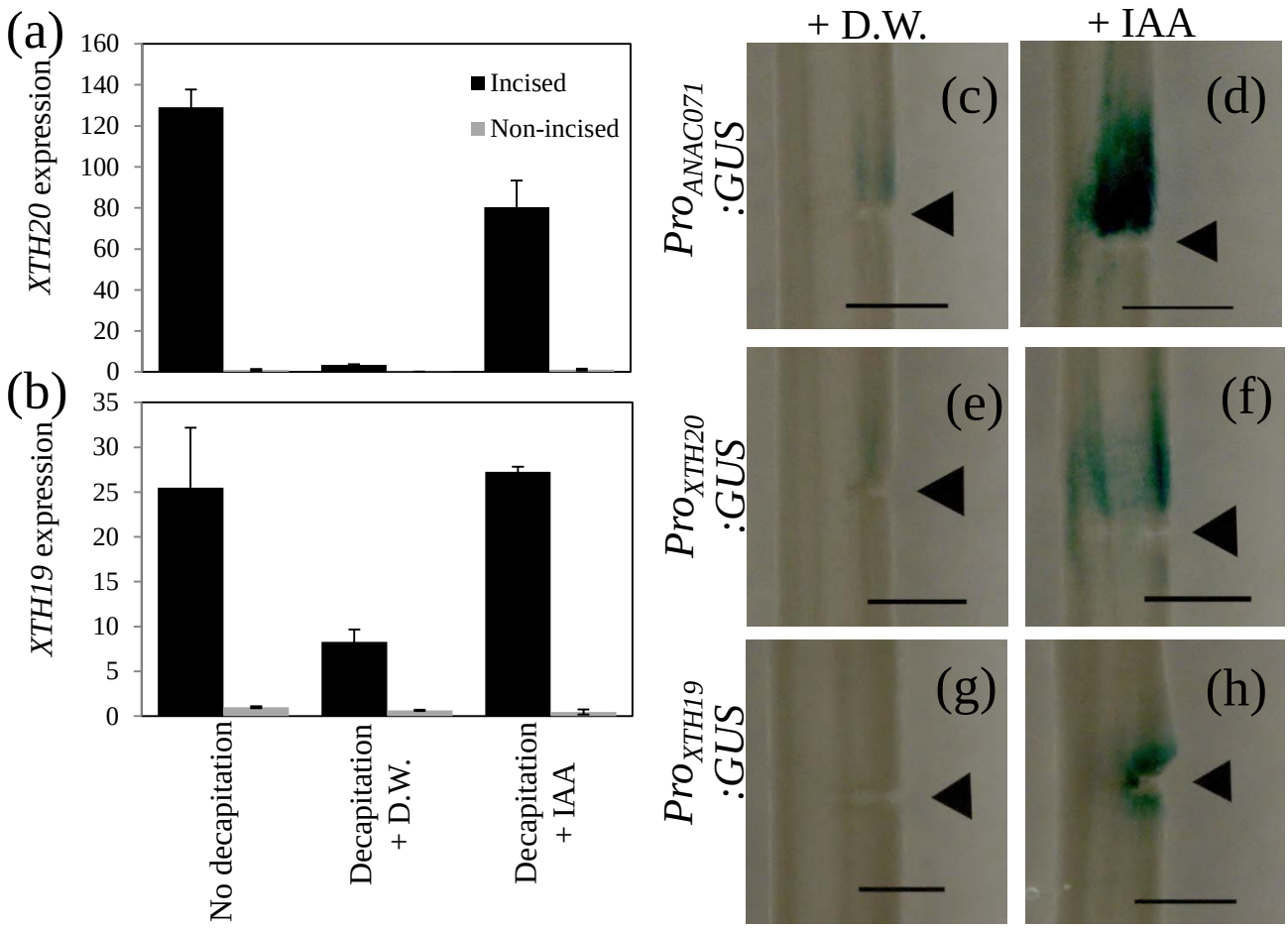

Figure 2. Effect of auxin on the induction of *ANAC071*, *XTH20*, and *XTH19* in the tissue reunion process.

(a,b) Expression levels of *XTH20* (a) and *XTH19* (b) in incised (black bar) and non-incised (gray bar) stems. The expression levels of *XTH20* and *XTH19* were examined by quantitative RT-PCR in non-decapitated plants and in decapitated plants 1 day after the incision was made after decapitation followed by the application of distilled water (D.W.) or 10^{-3} M IAA at the top of the cut stems. Mean ± SD (n = 3).

(c–h) Promoter activity of *ANAC071*, *XTH20*, and *XTH19*. GUS activity was detected 1 day after an incision was made in inflorescence stems of $Pro_{ANAC071}$*:GUS*, Pro_{XTH20}*:GUS*, and Pro_{XTH19}*:GUS* transgenic plants after decapitation followed by application of distilled water (D.W.) (c, e, and g) or 10^{-3} M IAA (d, f, and h). Bar = 0.5 mm.

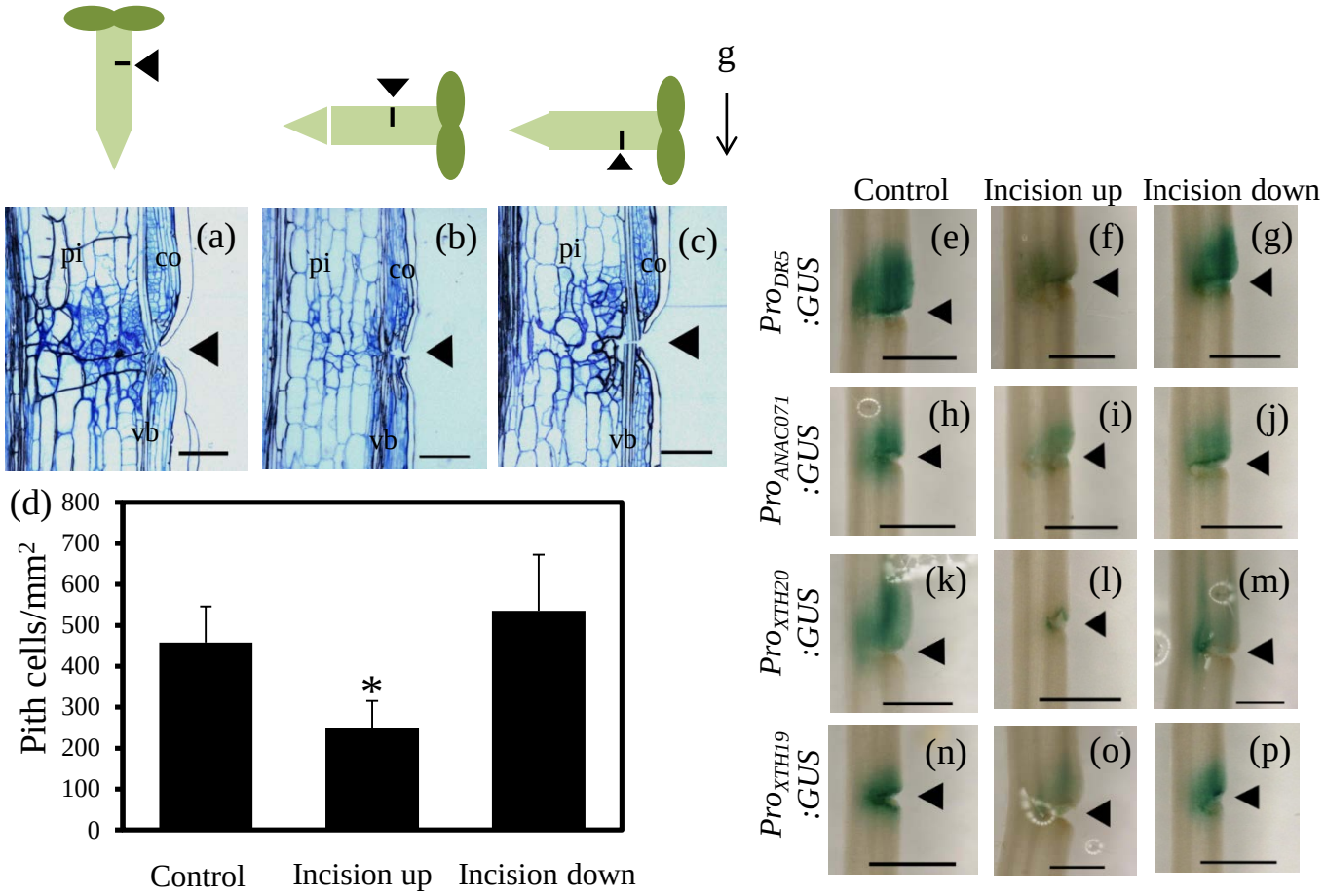

Figure 3. Effects of gravity on the tissue reunion process.

(a–c) Tissue reunion phenotypes observed 7 days after an incision was made in plants grown vertically (a) or horizontally with upward-facing (b) and downward-facing (c) incisions. Arrowheads indicate the position of the incision. g, gravity; pi, pith; co, cortex; vb, vascular bundle. Bar = 100 µm.

(d) Cell density in pith tissues calculated from sectioned samples as grown in (a–c). Mean ± SD (n = 7). *P < 0.05 (t-test). Calculation is described in Figure S5.

(e–p) Promoter activity of *DR5, ANAC071*, *XTH20*, and *XTH19*. GUS activity was detected in incised inflorescence stems of Pro_{DR5}*:GUS*, $Pro_{ANAC071}$*:GUS*, Pro_{XTH20}*:GUS*, and Pro_{XTH19}*:GUS* transgenic plants 3 days after an incision was made. Immediately after the incision was made, plants were oriented vertically as a control (e, h, k, and n) or horizontally with upward-facing (f, i, l, and o) or downward-facing (g, j, m, and p) incisions. Bar = 0.5 mm.

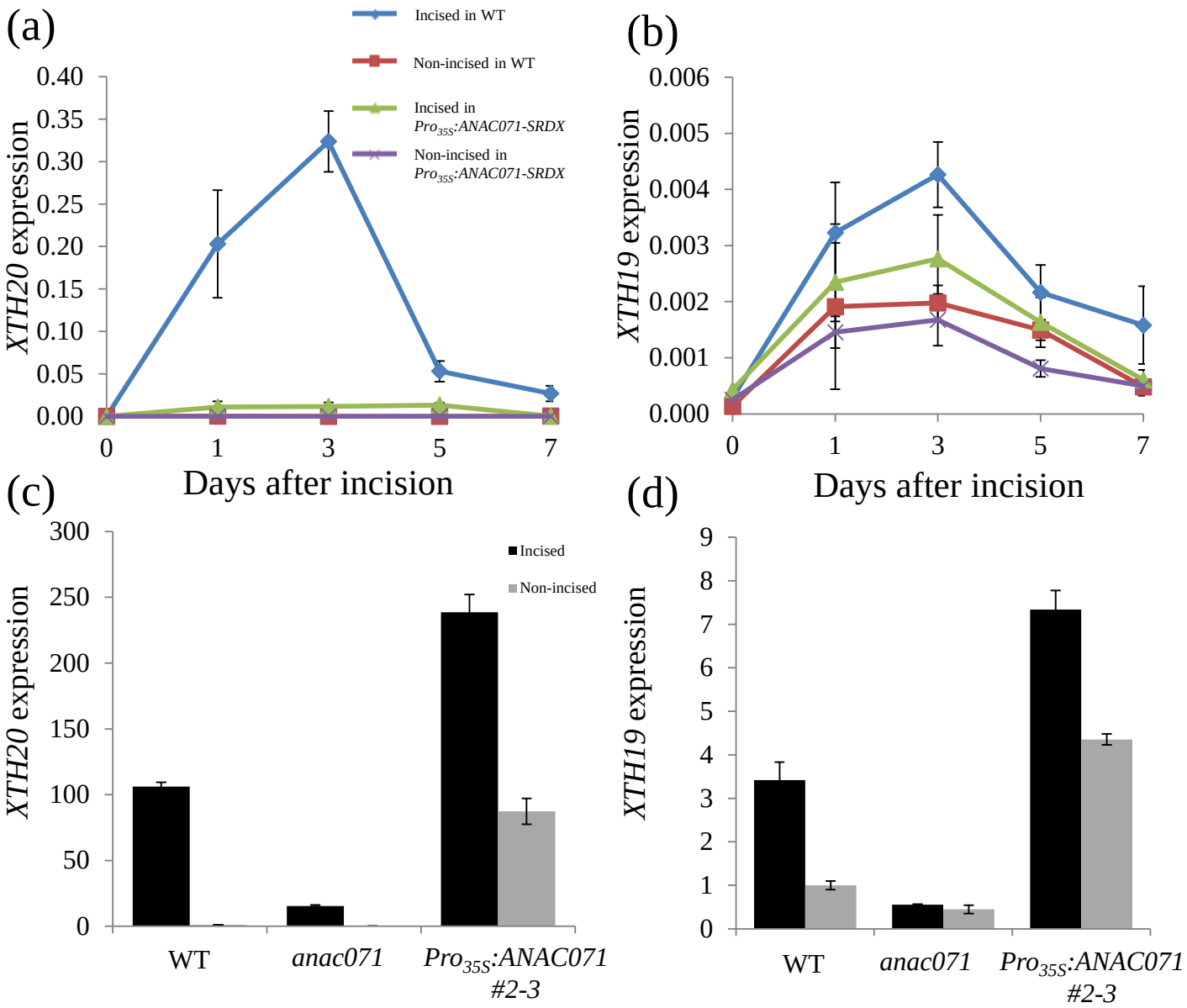

Figure 4. Control of the expression of *XTH20* and *XTH19* by *ANAC071* during the tissue reunion process.

(a,b) Expression of *XTH20* (a) and *XTH19* (b) was examined by quantitative RT-PCR in inflorescence stems of wild-type (incised = blue; non-incised = red) and *Pro$_{35S}$:ANAC071-SRDX* transgenic (incised = green; non-incised = purple) plants 0–7 days after the incision was made. Mean ± SD (*n* = 3).

(c,d) Quantitative RT-PCR analysis of *XTH20* (c) and *XTH19* (d) in incised (black bar) and non-incised (gray bar) inflorescence stems of wild-type, *anc071*, and *Pro$_{35S}$:ANAC071* transgenic plants 3 days after the incision was made. Mean ± SD (*n* = 3).

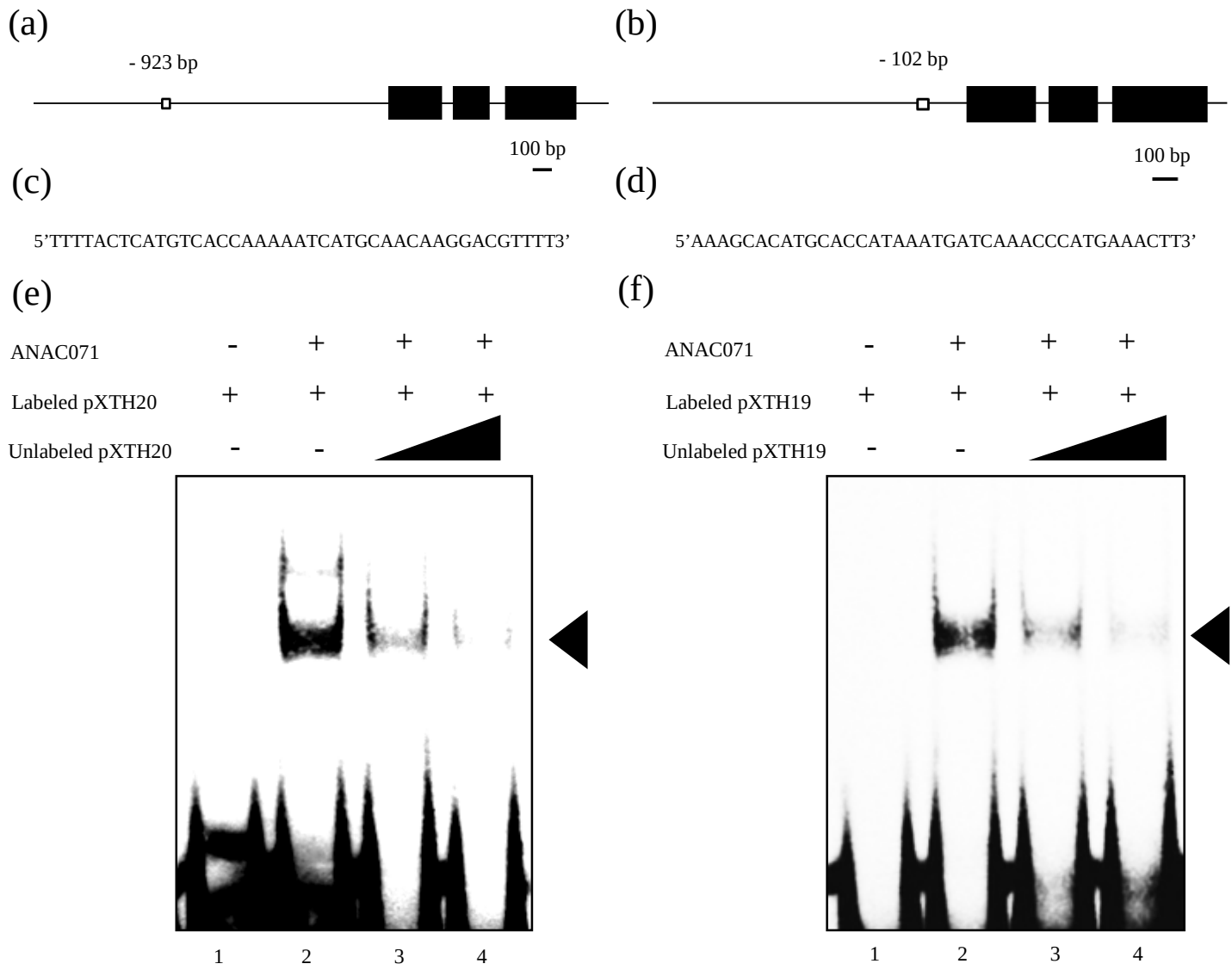

Figure 5. Binding of ANAC071 to *XTH20* and *XTH19* promoters.

(a,b) Illustration of selected oligonucleotides containing the *cis*-elements of the NAC recognition site (CATGT and CATG) and a presumed core binding site (CACC) in the promoters of *XTH20* (a) (–923 bp) and *XTH19* (b) (–102 bp). Black boxes indicate exons.

(c,d) Oligonucleotides used in the EMSA. The probes for *XTH20* (c) and *XTH19* (d) (pXTH20 and pXTH19, respectively) contained the *cis*-element of the NAC recognition site (CATGT and CATG) and the presumed core binding site (CACC) in the *XTH20* and *XTH19* promoter regions.

(e,f) The EMSA showed binding of His-ANAC071 to the CATGT, CACC, and CATG motifs in *XTH20* (e) and *XTH19* (f) promoters. Protein-DNA complexes were detected when His-ANAC071 fusion protein was incubated with labeled pXTH20 or pXTH19 probes (lane 2). Unlabeled pXTH20 or pXTH19 (lanes 3 and 4) were used for 100-fold (lanes 3) and 200-fold (lanes 4) excess levels of competitors. Arrowheads indicate the position of the protein-DNA complex.

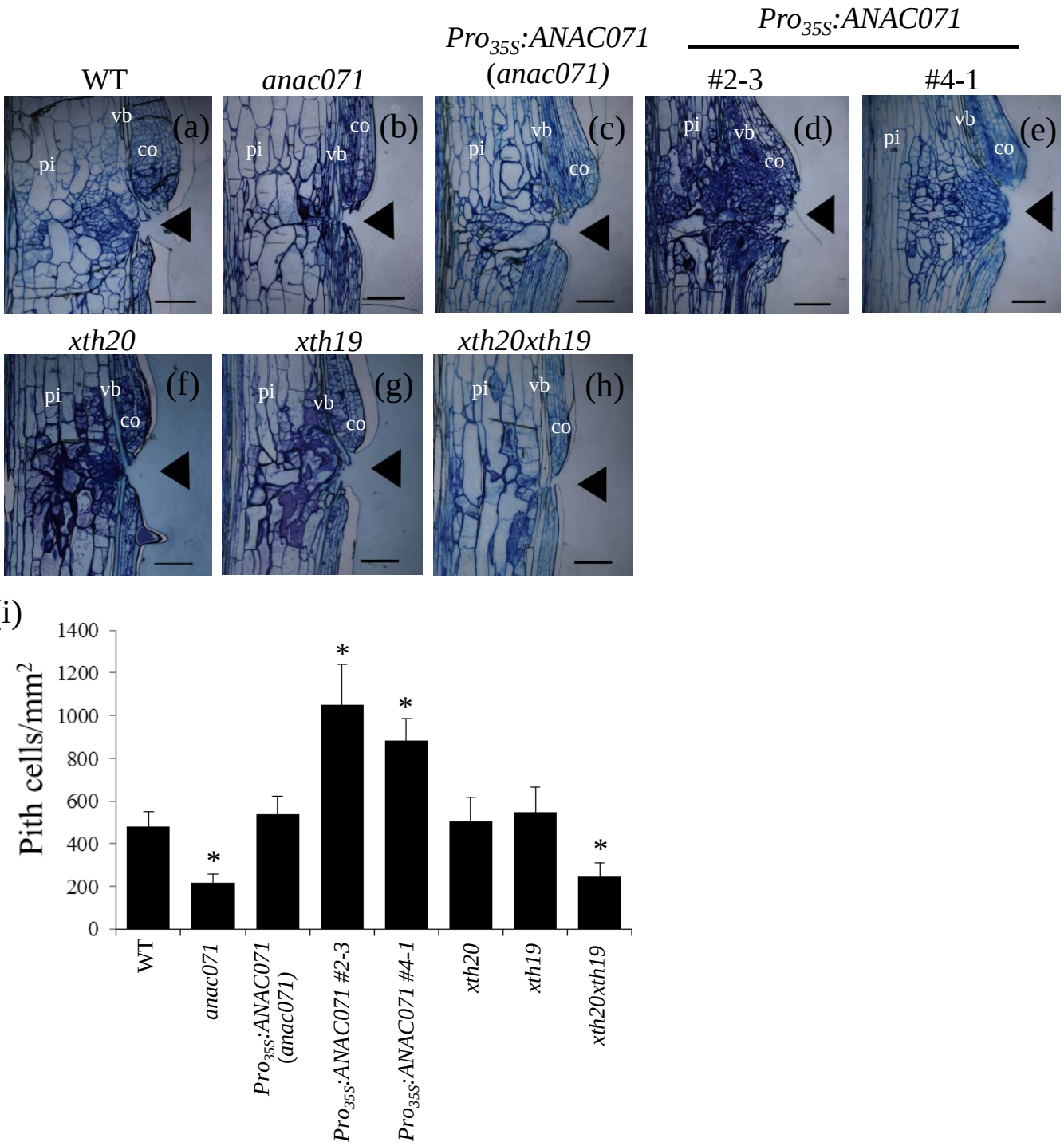

Figure 6. Phenotypes of *anac071*, *xth20*, and *xth19* single mutants and the *xth20xth19* double mutant and the effect of *ANAC071* overexpression on cell division in pith tissue.

(a–h) Tissue reunion phenotype observed 7 days after the incision was made. *Pro$_{35S}$:ANAC071* was introduced into *anac071* mutant (*Pro$_{35S}$:ANAC071* (*anac071*)) or two wild-type lines (*Pro$_{35S}$:ANAC071* #2-3 and #4-1). Arrowheads indicate the position of the incision. pi, pith; co, cortex; vb, vascular bundle; WT, wild type. Bar = 100 µm.

(i) Cell density in pith tissue was calculated from sectioned samples. Mean ± SD (n = 7). *P < 0.05 (t-test compared with WT).

Table S1 Monosaccharide composition in incised and non-incised inflorescence stems.

Fraction	Stem	Monosaccharide composition (mol%)						
		Ara	Rha	Fuc	Xyl	Man	Gal	Glc
α-amylase	Non-incised	18.0 ± 0.8	24.2 ± 1.6	5.2 ± 0.5	11.8 ± 0.5	1.2 ± 0.0	31.3 ± 0.8	8.2 ± 1.4
	Incised	23.0 ± 1.2*	23.3 ± 0.4	4.7 ± 0.1	11.1 ± 1.0	1.3 ± 0.1	31.1 ± 0.5	5.5 ± 0.3*
EPG	Non-incised	12.0 ± 2.0	14.9 ± 0.5	2.0 ± 0.5	38.0 ± 1.0	1.4 ± 0.1	21.7 ± 0.1	10.0 ± 1.6
	Incised	17.5 ± 0.7*	15.4 ± 0.9	1.7 ± 0.3	33.9 ± 2.1	1.4 ± 0.1	23.8 ± 1.1	6.3 ± 0.7*
Na_2CO_3	Non-incised	8.3 ± 0.5	7.7 ± 0.4	2.2 ± 0.1	38.7 ± 4.9	2.0 ± 0.3	24.4 ± 2.0	16.6 ± 7.4
	Incised	14.2 ± 2.6*	8.9 ± 0.3*	2.3 ± 0.4	38.7 ± 2.1	1.9 ± 0.2	27.3 ± 1.0	6.8 ± 0.2
1 M KOH	Non-incised	2.7 ± 0.1	1.7 ± 0.1	0.8 ± 0.2	84.3 ± 0.9	0.6 ± 0.0	2.8 ± 0.2	7.1 ± 0.8
	Incised	2.8 ± 0.8	1.7 ± 0.2	1.1 ± 0.1	84.5 ± 1.8	0.6 ± 0.1	3.2 ± 0.2	6.1 ± 1.1
4 M KOH	Non-incised	1.1 ± 0.2	1.2 ± 0.1	2.0 ± 0.2	66.4 ± 2.5	7.8 ± 0.6	5.9 ± 0.4	17.0 ± 1.4
	Incised	1.3 ± 0.2	1.3 ± 0.1	2.4 ± 0.2	65.6 ± 2.3	8.0 ± 0.2	6.2 ± 0.6	15.1 ± 1.6
Residue	Non-incised	4.4 ± 1.8	0.6 ± 0.2	0.4 ± 0.1	5.6 ± 2.2	ND	2.4 ± 0.4	86.5 ± 2.5
	Incised	5.7 ± 1.3	0.8 ± 0.1	0.7 ± 0.4	5.6 ± 1.2	ND	2.7 ± 0.2	84.5 ± 0.9

Neutral monosaccharide composition of incised or non-incised *Arabidopsis* stem segments (4 mm in length) sampled 7 days after the incision was made were analyzed by gas chromatography in cell wall polysaccharide fractions. Values are the mean ± SD from three biological samples. Asterisks indicate statistically significant differences between non-incised and incised stems (Student's *t*-test, $P < 0.05$). ND: not detected.

Table S2 Glycosyl-linkage composition of polysaccharides in the α-amylase fraction.

Glycosyl residue	Non-incised stem (mol%)	Incised stem (mol%)
T-Ara$_f$	4.8 ± 0.2	8.4 ± 0.6*
5-Ara$_f$	2.5 ± 0.2	4.0 ± 0.4*
2, 5-Ara$_f$	0.8 ± 0.1	1.2 ± 0.1*
3, 5-Ara$_f$	1.9 ± 0.2	3.3 ± 0.3*
T-Rha$_p$	0.7 ± 0.2	0.6 ± 0.1
2-Rha$_p$	8.2 ± 0.3	7.1 ± 0.7
2, 3-Rha$_p$	1.0 ± 0.1	0.7 ± 0.0*
2, 4-Rha$_p$	6.7 ± 0.6	8.8 ± 0.3*
2, 3, 4-Rha$_p$	10.6 ± 0.8	8.6 ± 0.4*
T-Fuc$_p$	1.1 ± 0.0	1.7 ± 0.6
3, 4-Fuc$_p$	2.5 ± 0.2	1.9 ± 0.3*
T-Xyl$_p$	4.2 ± 0.4	4.2 ± 0.6
2-Xyl$_p$	0.4 ± 0.0	1.0 ± 0.1*
4-Xyl$_p$	1.8 ± 0.2	1.0 ± 0.1*
T-Gal$_p$	6.5 ± 0.2	5.8 ± 0.8
2-Gal$_p$	0.4 ± 0.1	0.3 ± 0.0*
4-Gal$_p$	1.3 ± 0.4	1.6 ± 0.1
6-Gal$_p$	5.6 ± 1.5	4.2 ± 0.3
2, 4-Gal$_p$	1.4 ± 0.2	1.0 ± 0.2
3, 6-Gal$_p$	1.9 ± 0.5	4.3 ± 2.5
T-Glc$_p$	1.5 ± 0.1	1.3 ± 0.2
4-Glc$_p$	3.4 ± 0.2	2.6 ± 0.2*
4-Gal$_p$A	15.1 ± 0.6	12.6 ± 1.4*
2, 4-Gal$_p$A	2.6 ± 0.3	1.4 ± 0.1*
3, 4-Gal$_p$A	4.8 ± 0.2	2.8 ± 0.1*
2, 3 ,4-Gal$_p$A	8.4 ± 0.4	9.5 ± 1.0

Glycosyl-linkage composition of polysaccharides in the α-amylase fraction of incised or non-incised *Arabidopsis* stem segments (4 mm in length) sampled 7 days after the incision was made were analyzed by gas chromatography–mass spectrometry. Values are the mean ± SD from three measurements. Asterisks indicate statistically significant differences between non-incised and incised stems (Student's *t*-test, $P < 0.05$).

Table S3 Primers used in this research

Name of primer	DNA sequence (5' to 3')
Plasmid construction	
Pro$_{ANAC071}$:GUS	
F pANAC071	CACCGAAATCGTCCAGCCATAATTGG
R pANAC071	TGCAAAATTCACACTTGTAGCTTGC
Pro$_{35S}$:ANAC071	
F OX-ANAC071	CACCATGGGGAGTTCATGTTTGCCTC
R OX-ANAC071	CTAAGAACGAACCAACATTTCTTGT
Detection of T-DNA insertion	
F-*anac071* (SALK_012841C)	CGCATGTTATAGCTGGAT
R-*anac071* (SALK_012841C)	CTAAGAACGAACCAACATTTCTTGT
F-*xth20* (SALK_066758)	GGATGAAATAGATTTTGAGTT
R-*xth20* (SALK_066758)	CAGTGCAATAGTTGTAGACC
F-*xth19* (GK369E06.01)	ATGAAGTCTTTTACGTTCTTG
R-*xth19* (GK369E06.01)	GACTTTCCATTAACCCATAC
LBb1	GCGTGGACCGCTTGCTGCAACT
LB1-GABI	CTTTCTTTTTCTCCATATTGACCATCA
Primer for qRT-PCR analysis	
F ANAC071	CCTCTCCTTGTCGCGATGAA
R ANAC071	ATGCTTGAAGAGTCGTTTGTAGTAGAAG
F XTH20	TAATCACGTGGCATTGTCTTTGTA
R XTH20	AATTTATTTAGCGCAAATACTCAGCTAG
F XTH19	TGCAGCTAAATGATTGATTCTTTGAT
R XTH19	CCATTGAGTTACAAAGACAACGCAA
F ACT7	CAGTGTCTGGATCGGAGGAT
R ACT7	TGAACAATCGATGGACCTGA
Primer for EMSA	
ANAC071-His-tag construction	
F ANAC071-pCold	GGAGGCCAGTGAATTCATGGGGAGTTCATGTTTGCCTC
R ANAC071-pCold	TCATCTGCAGCTCGAGCTAAGAACGAACCAACATTTCTTGT

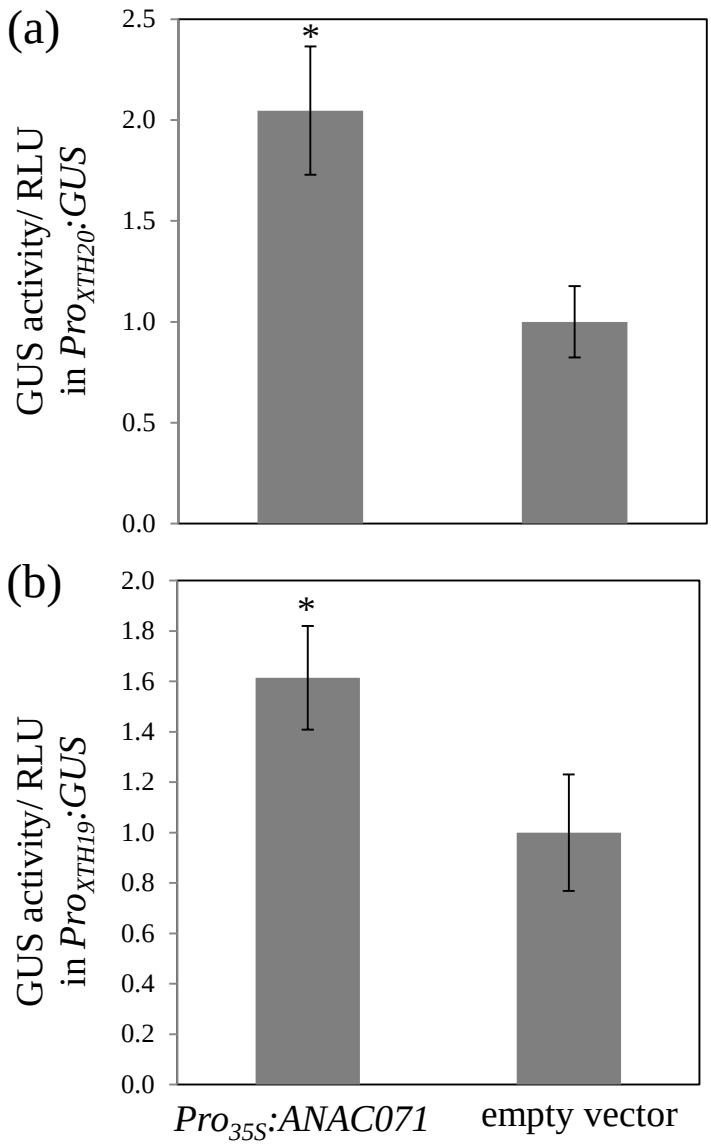

Figure S1. Effects of transient expression of *ANAC071* on the expression of *XTH20* and *XTH19* in the leaves of Pro_{XTH20}*:GUS* and Pro_{XTH19}*:GUS* transgenic plants.
(a,b) GUS activity after infiltration of *Agrobacterium* harboring pK2GW7 containing Pro_{35S}*:ANAC071* or empty pK2GW7 vector and pCAMBIA containing Pro_{35S}*:Luciferase* (internal control) into Pro_{XTH20}*:GUS* (a) or Pro_{XTH19}*:GUS* (b) transgenic plants. Mean ± SD (n = 10). GUS activity and the relative light unit (RLU) for luciferase activity were measured 3 days after infiltration. Asterisks indicate statistically significant differences between Pro_{35S}*:ANAC071* and empty vector (Student's t-test, $P < 0.05$).

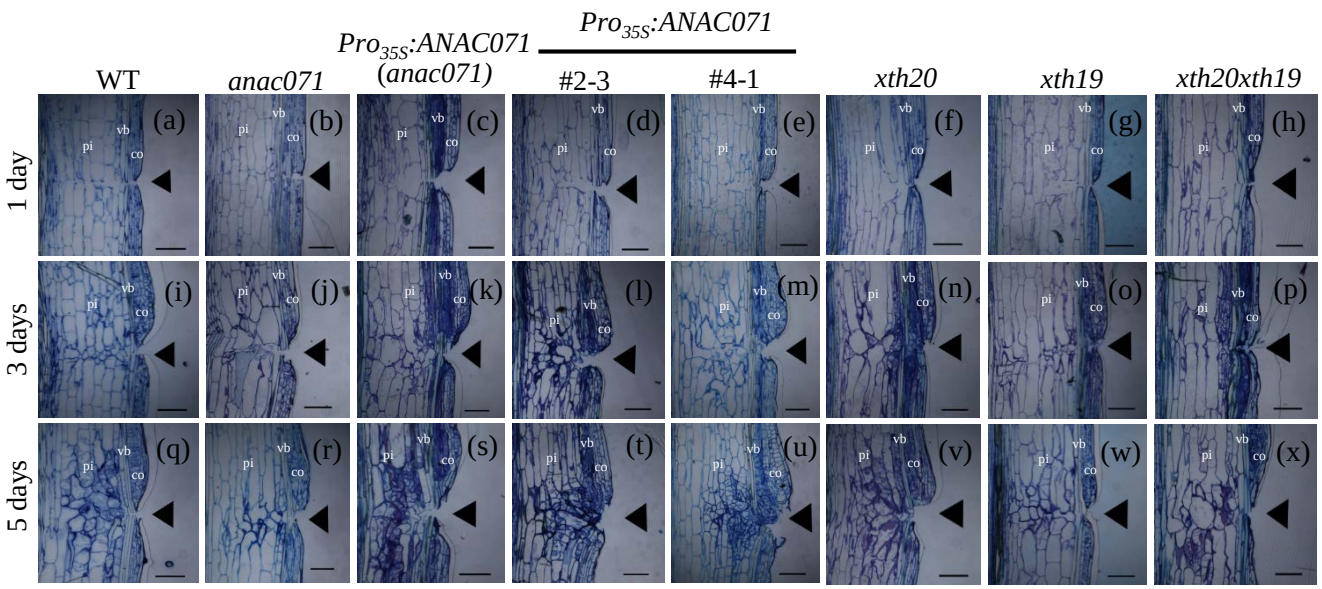

Figure S2. Tissue reunion phenotypes at 1, 3, and 5 days after the incision was made.

(a–x) Tissue reunion phenotype of wild type (a, i, q), *anac071* (b, j, r), *Pro$_{35S}$:ANAC071* in the *anac071* background (c, k, s), *Pro$_{35S}$:ANAC071* transgenic lines #2-3 (d, l, t) and #4-1 (e, m, u), *xth20* (f, n, v) and *xth19* (g, o, w) single mutants, and the *xth20xth19* double mutant (h, p, x) 1 day (a–h), 3 days (i–p), and 5 days (q–x) after the incision was made. Arrowheads indicate positions of the incision. pi, pith; co, cortex; vb, vascular bundle. Bar = 100 µm. Three plants for each genotype were examined, and representative photographs are shown.

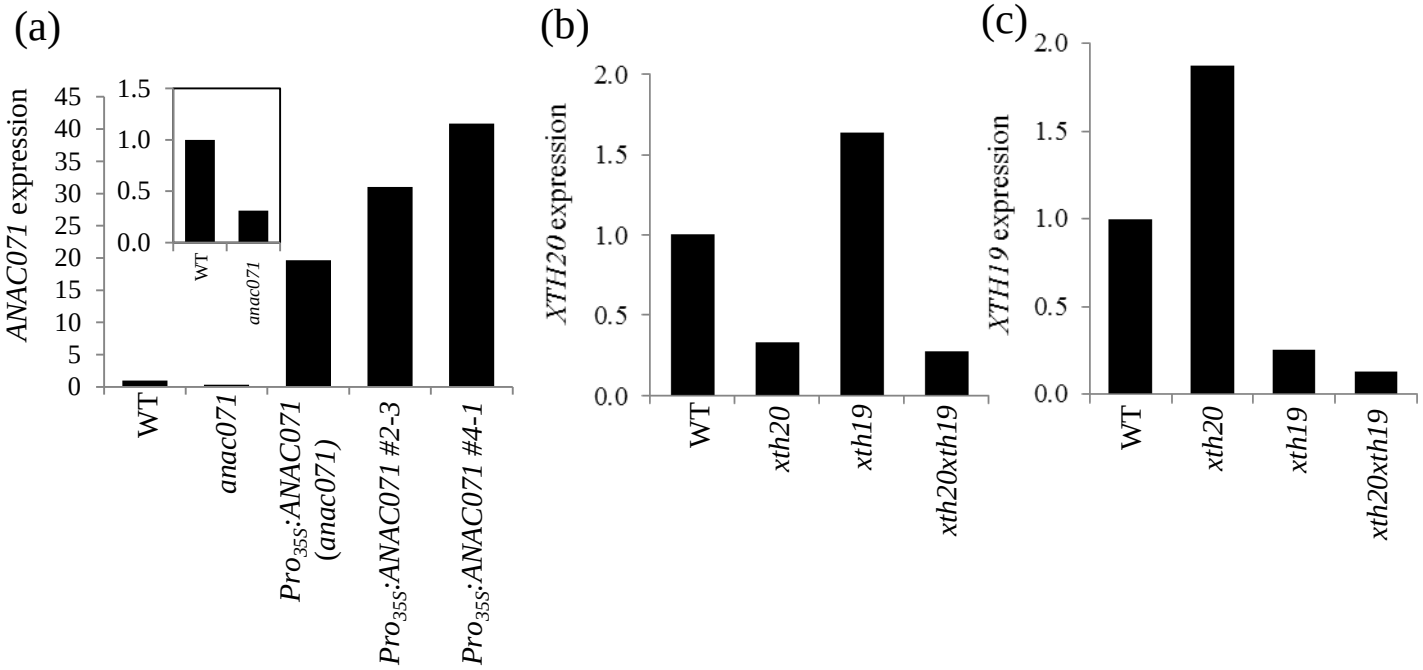

Figure S3. Expression level of *ANAC071*, *XTH20*, and *XTH19*.

(a–c) Expression level of *ANAC071* (a), *XTH20* (b), and *XTH19* (c) in *anac071*, *Pro$_{35S}$:ANAC071* in the *anac071* background, *Pro$_{35S}$:ANAC071* transgenic lines (#2-3 and #4-1), *xth20* and *xth19* single mutants, and the *xth20xth19* double mutant as compared with wild-type plants. WT, wild type.

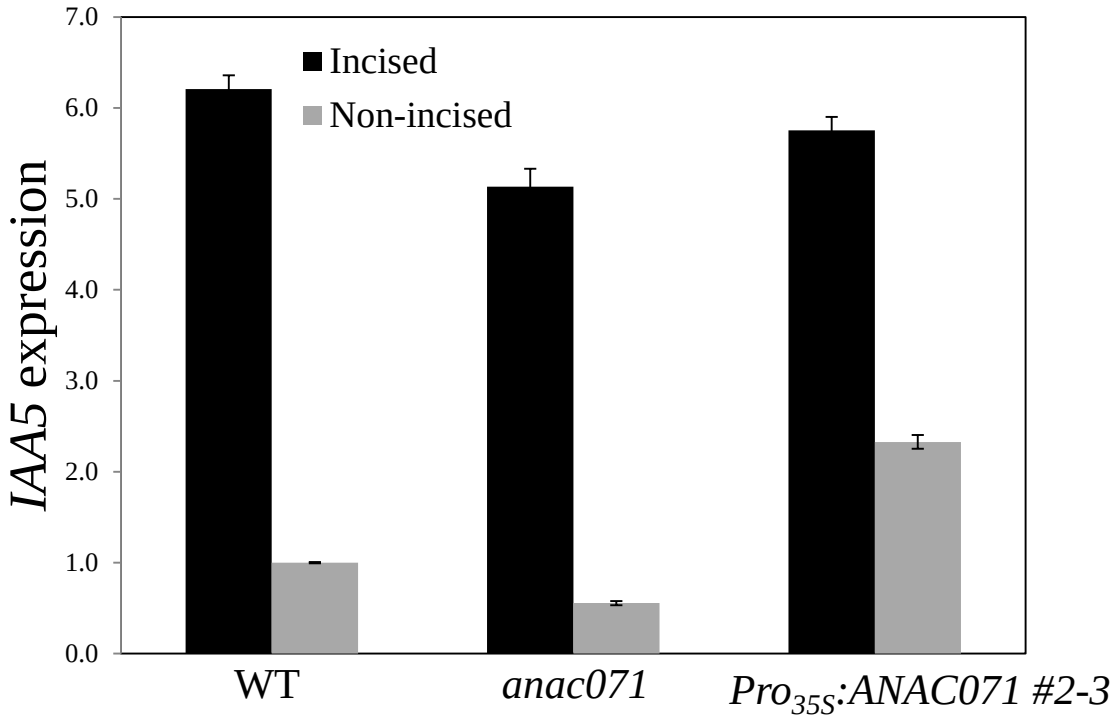

Figure S4. Expression of *IAA5* in incised and non-incised stems of wild-type, *anac071*, and *Pro$_{35S}$:ANAC071* transgenic plants.

Expression levels of *IAA5* in incised (black bar) and non-incised (gray bar) stems 1 day after the incision was made. Mean ± SD (*n* = 3). WT, wild type.

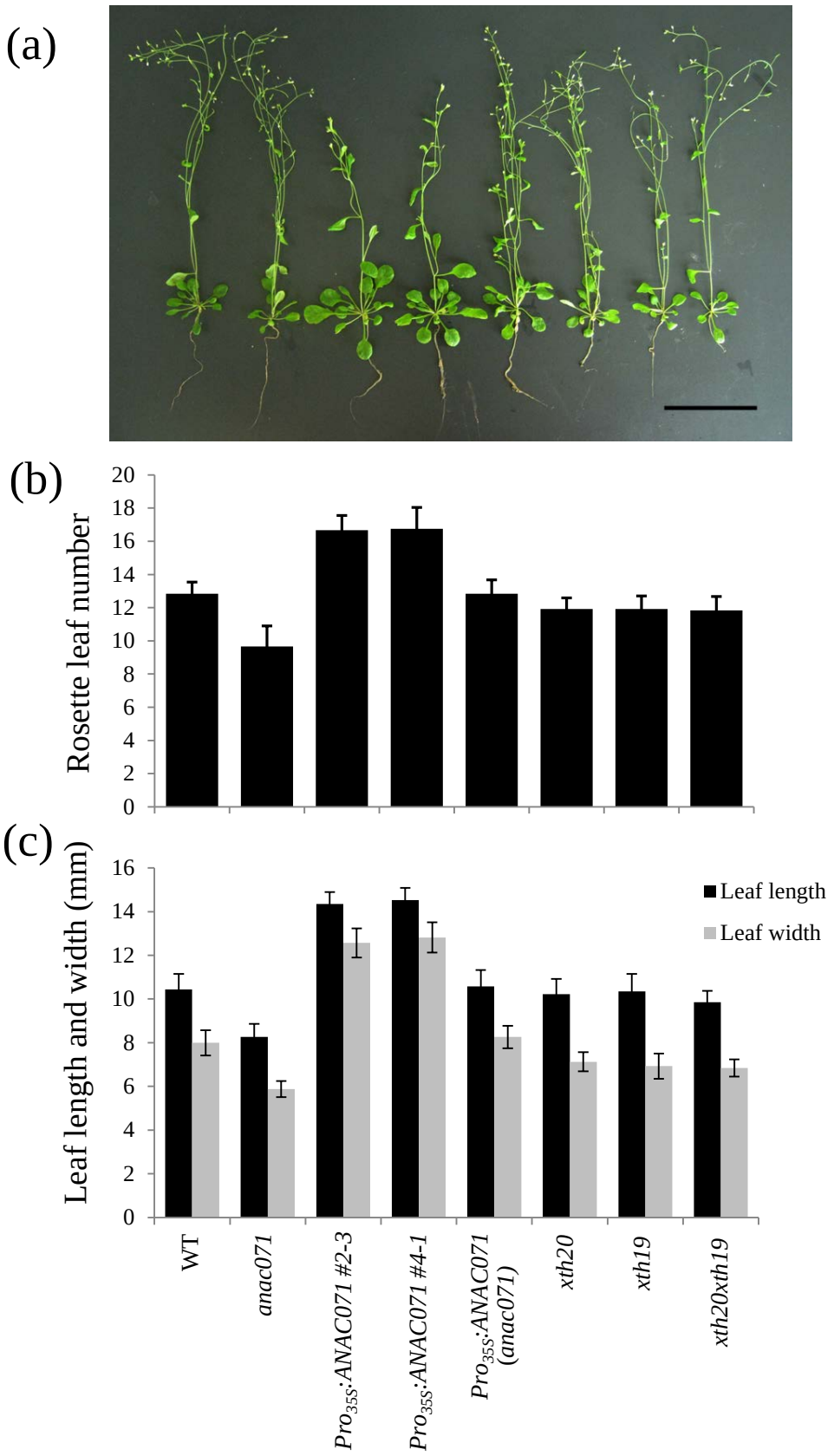

Figure S5. Morphology of plants.

(a) Photograph of wild-type, *anac071*, *Pro$_{35S}$:ANAC071* transgenic wild-type lines (#2-3 and #4-1), *Pro$_{35S}$:ANAC071* in the *anac071* background, *xth20* and *xth19* single mutants, and the *xth20xth19* double mutant (from left to right). Bar = 5 cm.

(b) Rosette leaf number in mature plants (3 weeks after transfer to soil). Mean ± SD (*n* = 12).

(c) Leaf length (black bar) and width (gray bar) of the sixth rosette leaf. Mean ± SD (*n* = 12). WT, wild type.

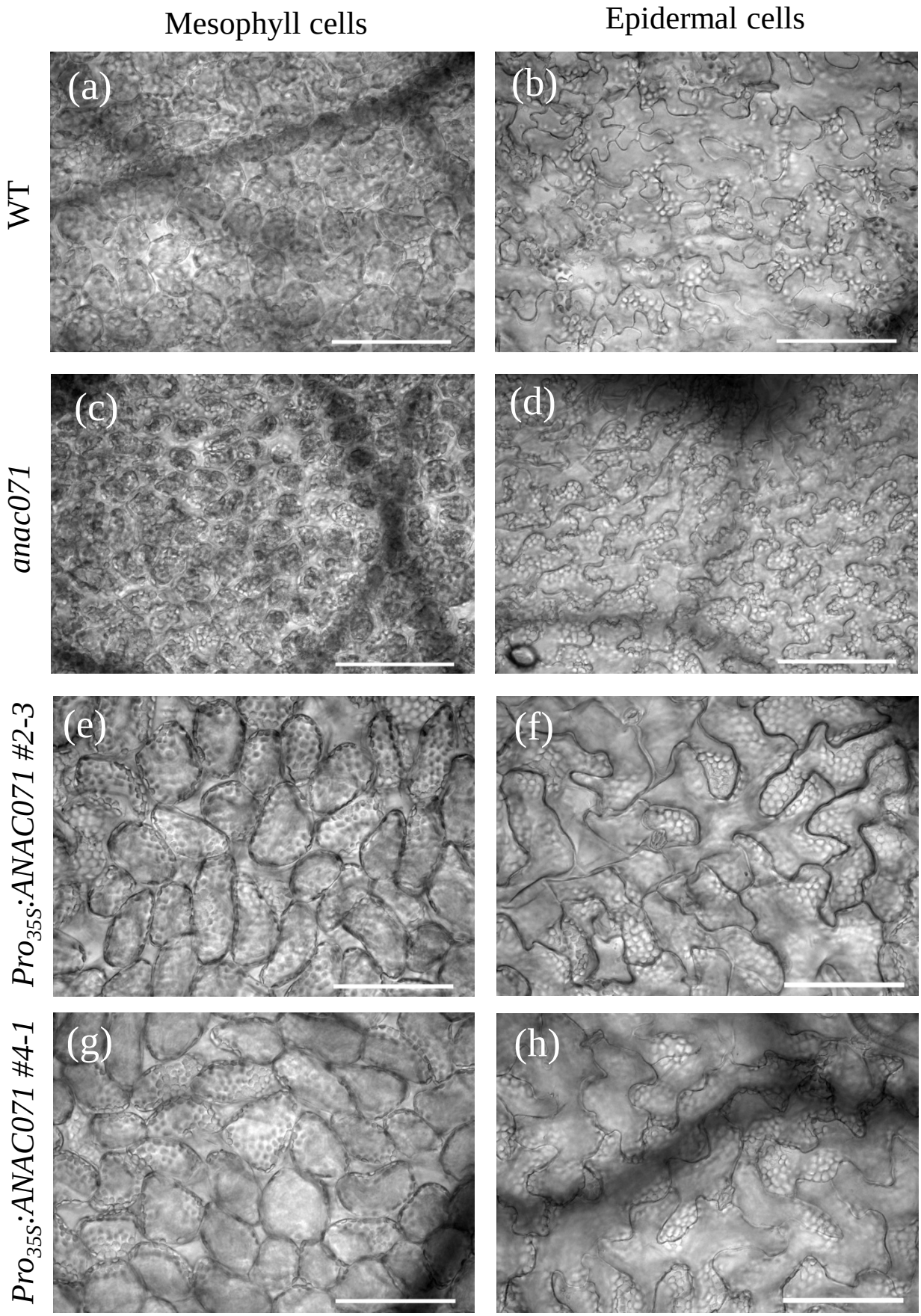

Figure S6. Mesophyll and epidermal cells of wild-type, *anac071*, and *Pro35S:ANAC071* transgenic plants.

(a,c,e,g) Mesophyll cells of wild type (a), *anac071* (c), *Pro35S:ANAC071* transgenic line #2-3 (e), and *Pro35S:ANAC071* transgenic line #4-1 (g). Bar = 100 μm.

(b,d,f,h) Epidermal cells of wild type (b), *anac071* (d), *Pro35S:ANAC071* transgenic line #2-3 (f), and *Pro35S:ANAC071* transgenic line #4-1 (h). Bar = 100 μm. WT, wild type.

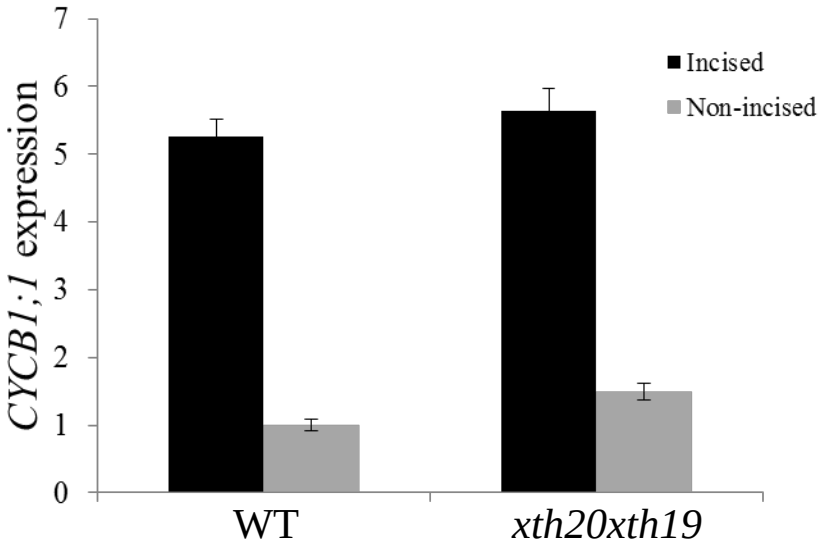

Figure S7. Expression of *CYCB1;1* in incised and non-incised stems of wild type and *xth20xth19*. Expression levels of *CYCB1;1* in incised (black bar) and non-incised (gray bar) stems 3 days after the incision was made. Mean ± SD (*n* = 3). WT, wild type.

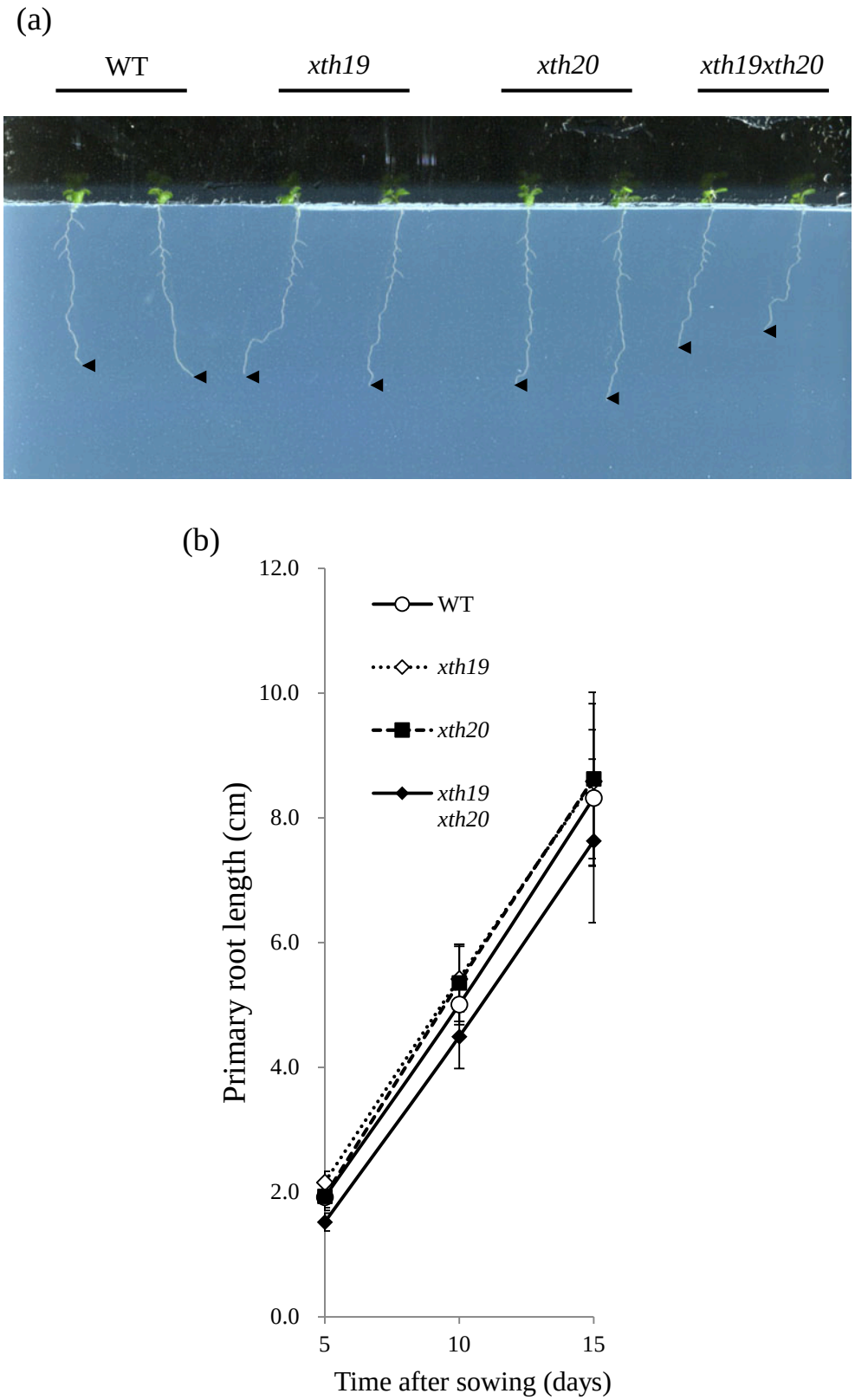

Figure S8. Primary root length of the XTH mutants.

(a) Photograph of wild-type and XTH mutant roots 10 days after sowing plants in half-strength MS medium. Arrowheads indicate root tips.

(b) Primary root length of wild-type (white circle), *xth19* (white diamond), *xth20* (black square), and *xth20xth19* (black diamond) plants 5, 10, and 15 days after sowing. Mean ± SD (n = 12). WT, wild type.

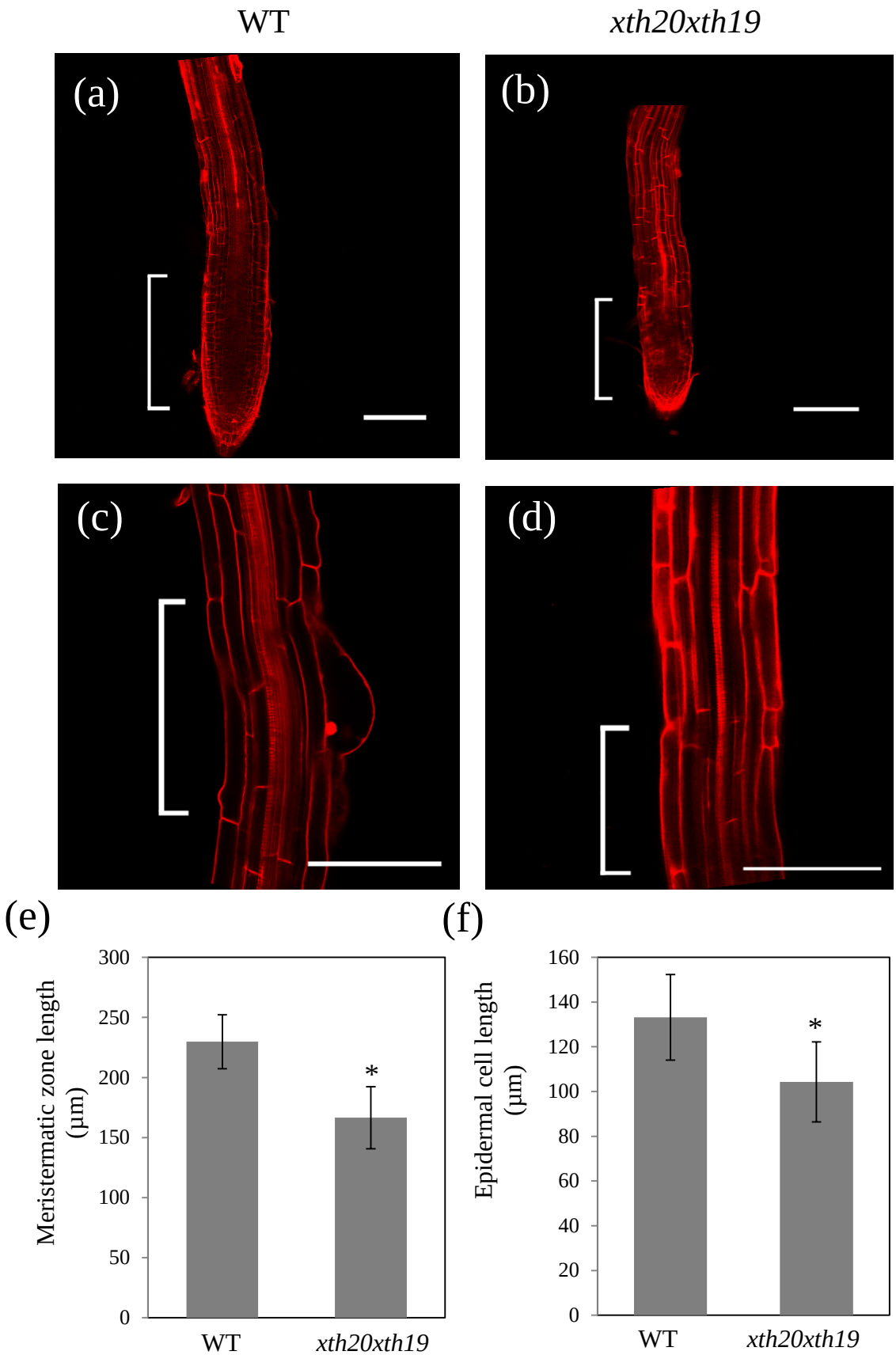

Figure S9. Meristematic zone and epidermal cells of wild-type and *xth20xth19* roots.

(a–d) Meristematic zone (a,b) and epidermal cells (c,d) of roots of wild type (a,c) and *xth20xth19* (b,d) 10 days after sowing. Bar = 200 μm (a,b) and 100 μm (c,d). Roots were stained with 10 mg/mL propidium iodide for 5 min and observed with a confocal laser-scanning microscope (LSM 710; Carl Zeiss, Germany).

(e,f) Meristematic zone length (e) and epidermal cell length (f) of roots of wild type and *xth20xth19* 10 days after sowing. Mean ± SD (n = 8). Asterisks indicate statistically significant differences between *xth20xth19* and wild type (Student's t-test, $P < 0.05$). WT, wild type.

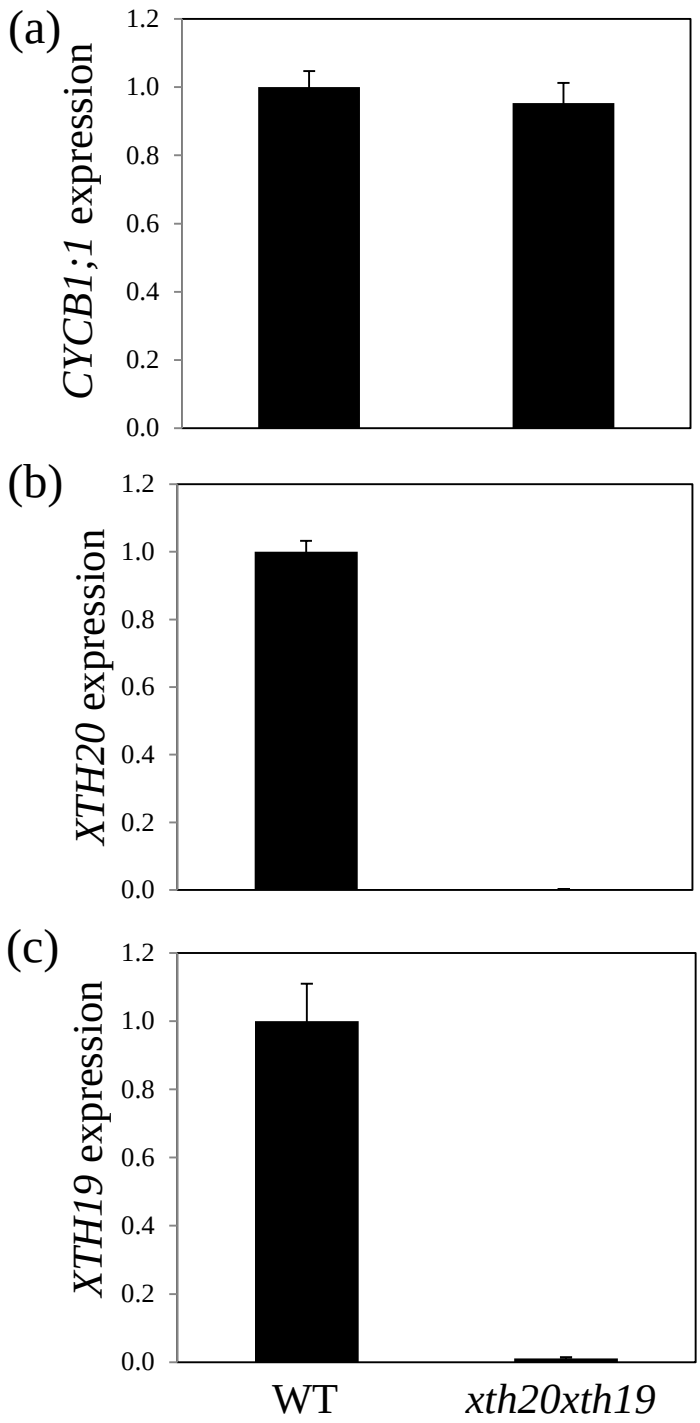

Figure S10. Expression of *CYCB1;1*, *XTH20*, and *XTH19* in roots of wild type and *xth20xth19*.
(a–c) Expression level of *CYCB1;1* (a), *XTH20* (b), and *XTH19* (c) of wild-type and *xth20xth19* roots 10 days after sowing. Mean ± SD (*n* = 3).

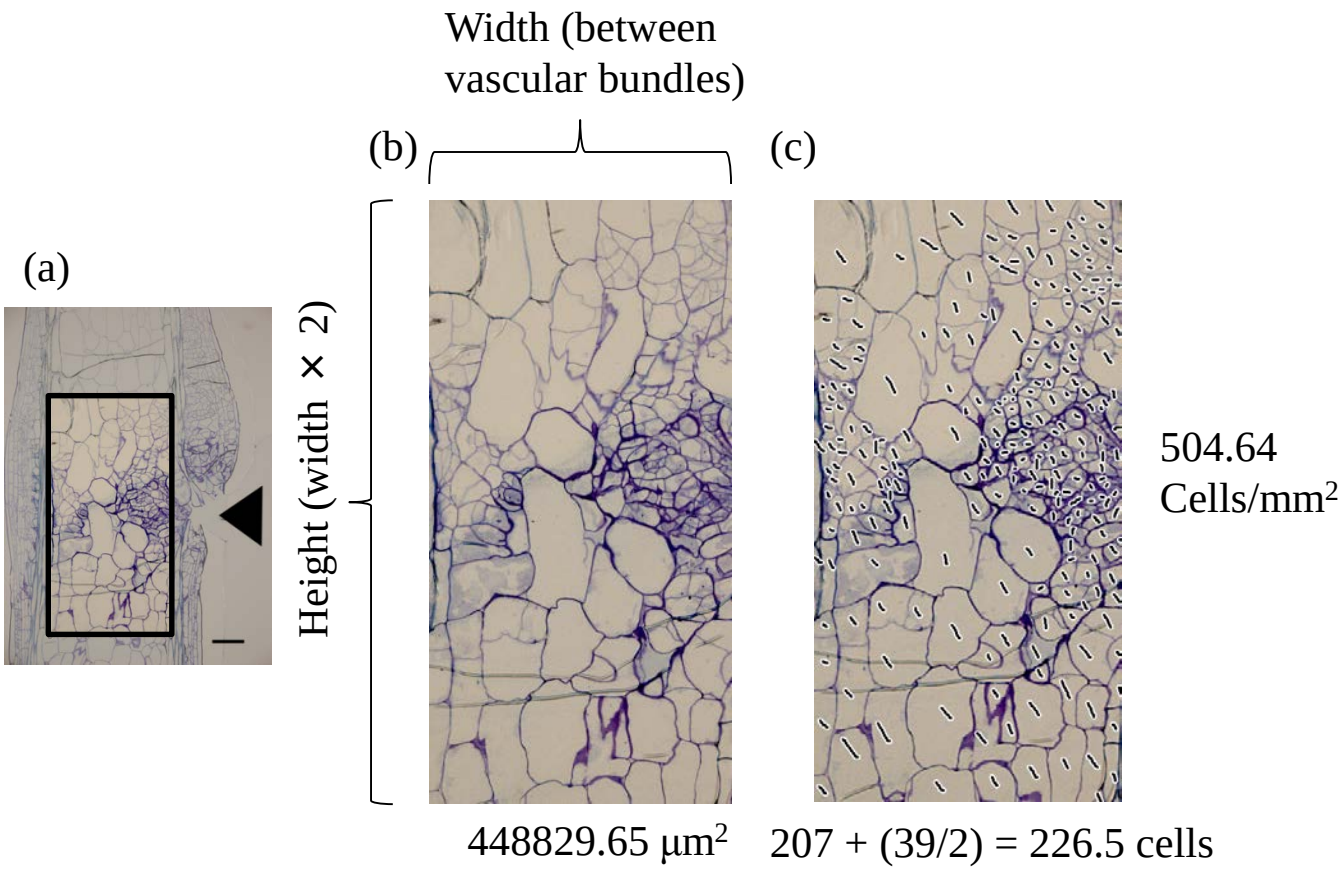

$$\text{Average cell number} = \left\{ \text{Number of complete cells} \right\} + \left\{ \frac{\text{Number of partial cells}}{2} \right\}$$

Figure S11. Method for cell density calculation.

(a) Selected rectangle of pith tissue around the incision site for cell counting, with width (between vascular bundles) and height (width × 2). Bar = 100 µm.

(b) The selected area was measured with ImageJ software.

(c) Average cell number was counted manually based on the formula shown. The partial cells refer to those that were touching an edge of the rectangle.